ELSEVIER

ADVANCES IN COLLOID AND INTERFACE SCIENCE

Advances in Colloid and Interface Science
85 (2000) 103–144

www.elsevier.nl/locate/cis

Dynamic surface tension and adsorption mechanisms of surfactants at the air–water interface

J. Eastoe*, J.S. Dalton

University of Bristol, School of Chemistry, Cantock's Close, Bristol BS8 7TS, UK

Abstract

Recent advances in understanding dynamic surface tensions (DSTs) of surfactant solutions are discussed. For pre-CMC solutions of non-ionic surfactants, theoretical models and experimental evidence for a mixed diffusion–kinetic adsorption mechanism are covered. For micellar solutions of non-ionics, up to approximately 100 × CMC, the DST behaviour can also be accounted for using a mixed mechanism model. Finally, the first reported measurements of the dynamic surface excess $\Gamma(t)$, using the overflowing cylinder in conjunction with neutron reflection, are described.

Keywords: Dynamic surface tension; Adsorption mechanisms; Surfactant adsorption

Contents

* Corresponding author. Tel.: +44-117-928-9180; fax: +44-117-925-0612.
E-mail address: julian.eastoe@bris.ac.uk (J. Eastoe).

0001-8686/00/$ - see front matter
PII: S0001-8686(99)00017-2

1. Overview

The equilibrium surface tension (γ_{eq}) of a surfactant solution is not achieved instantaneously. For example, when a fresh interface is formed, surfactant molecules must first diffuse from the bulk to the interface, and then adsorb, whilst also achieving the correct orientation. The main question discussed here is 'what is (are) the main process(es) governing the rate of transport of surfactant molecules

from the bulk to the adsorbed state at the air–water interface'? The dynamic surface tensions (DSTs or $\gamma(t)$) can be measured by a variety of techniques such as maximum bubble pressure, drop volume or an inclined plate flow cell [1–4]. The rate of surfactant adsorption, or the change in surface excess concentration with time $\Gamma(t)$, can be inferred from the tension decay by applying an appropriate isotherm. However, a recent, and significant, advance has been the direct measurement of $\Gamma(t)$ by neutron reflection, and results for the cationic CTAB are described here.

The following introduction gives an insight into experimental and theoretical aspects of DST. Also included are suggested processes and parameters which may control adsorption dynamics, some of which are currently under debate.

1.1. Introduction to DST

A freshly formed interface of a surfactant solution has a surface tension, γ, very close to that of the solvent, γ_0. Over a period of time, γ will decay to the equilibrium value, γ_{eq}, and this period of time can range from milliseconds to days depending on the surfactant type and concentration. This dynamic surface tension (DST or $\gamma(t)$) is an important property as it governs many important industrial and biological processes [1–4]. For example, in the photographic industry the formulation of thin gelatin films requires high flow velocities, and hence DST needs to be monitored during the fabrication process to prevent film deformation and irregularities. It is also of importance in agrochemicals where fast wettability plays a role in the easy spreading of pesticides onto leaves. DST also plays a crucial part in metal, paper and textile production. One biological process where the control of DST is essential is in the lung, where DST is necessary for effective functioning of the alveoli, and phospholipids are the main surface active ingredients. It is, of course, important in other emulsifiers, wetting agents and foaming agents. Indeed, whenever surfactants are used, DST is an important property. Recent advances in experimentation and theory, which are covered here, have been the stimuli for a resurgence in this area.

For a surfactant solution at equilibrium, the interfacial (or surface excess) concentration of surfactant is given by Γ_{eq}. However, adsorption is a dynamic phenomenon, and at equilibrium the adsorbing flux of monomers to the surface, j_{ads}, is equal to the desorbing flux, j_{des}. This is shown in Fig. 1. If a surface is stretched, say by creating a liquid drop or by forming an air bubble in a liquid, the surface excess concentration, Γ, immediately after the perturbation will now be less than Γ_{eq}. Therefore, to re-establish equilibrium the adsorbing flux j_{ads} will now be greater than the desorbing flux, j_{des}, and in order to obtain equilibrium, there will be an overall transport of monomer from the bulk to the interface.

If the equilibrium surface is contracted, then $\Gamma > \Gamma_{eq}$ and therefore $j_{des} > j_{ads}$ in order to re-establish equilibrium, and there will be an overall transport of adsorbed monomer from the surface into the bulk (back diffusion). A simple relationship describing this kinetic mechanism is described in Eq. (1).

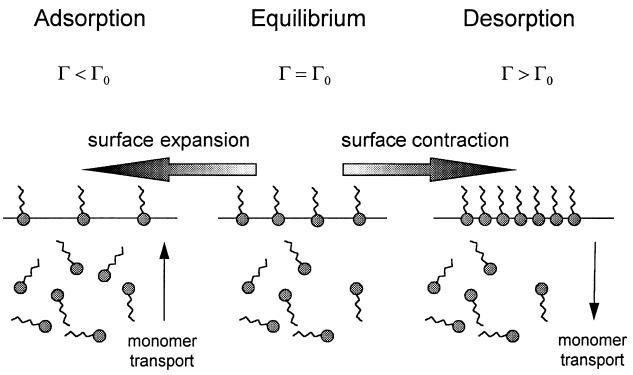

Fig. 1. Surface expansion and contraction may drive the flux of monomer to the interface.

$$\frac{d\Gamma}{dt} = j_{ads} - j_{des} \tag{1}$$

As stated, when a fresh surface is created, initially the surface excess of monomer is less than the equilibrium value, and since $\Gamma < \Gamma_{eq}$ there will be a flux of monomer from the bulk to the interface. This flux will cause the surface tension to decay from γ_0 to γ_{eq}, where the interfacial concentration has reached its equilibrium value, i.e. Γ_{eq}. Broadly speaking there are two main models for monomer transport and adsorption, and these are conveyed diagramatically in Fig. 2. The subsurface may be taken as an imaginary plane, a few molecular diameters below the interface.

These models are:

1. *diffusion controlled* which assumes the monomer diffuses from the bulk into the subsurface, and once in the subsurface it directly adsorbs at the interface. In this model the diffusion process from the bulk to subsurface is the rate-controlling step, and the timescale of adsorption from the subsurface to the interface is very fast. This model is discussed in Section 4.1.
2. The *mixed kinetic-diffusion* model assumes that the monomer diffuses from the bulk to the subsurface, but the rate-controlling process is transfer of these monomers to the interface. Once the monomer has diffused to the subsurface, there may be an adsorption barrier present preventing the monomer from adsorbing. This barrier may be due to increased surface pressure, or attributed to there being less 'vacant sites' available for adsorption. There may also be steric restraints on the molecule in the proximity of the interface, and it may have to be in the correct orientation to adsorb. This will cause the molecule to back diffuse into the bulk rather than adsorbing, thereby increasing the timescale of the DST decay. This model is discussed in Section 4.2.

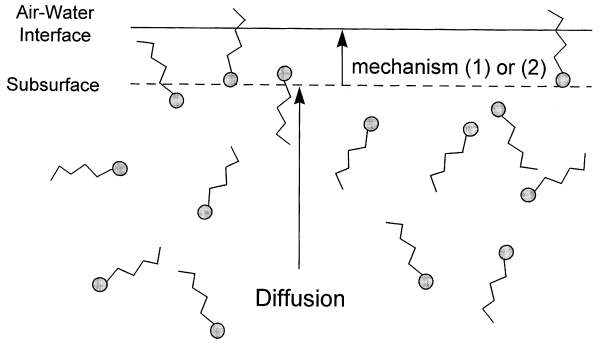

Fig. 2. Transport of monomer to the interface. Once the monomer has diffused to the subsurface it will either instantaneously adsorb at the interface in accordance with the diffusion-controlled model (1) or will have to pass through a potential barrier to adsorb (2).

Before the discussion of adsorption dynamics, it is important to cover relevant details of equilibrium adsorption behaviour. In addition, for any adsorption study it is of paramount importance that the equilibrium properties of the surfactants are well characterised. The purpose of Section 2 is to give a brief review of the common equilibrium adsorption isotherms and also the various methods used for measuring the equilibrium surface excess.

2. The interfacial concentration and methods of measurement

2.1. Thermodynamics of adsorption: the Gibbs equation

Assuming that activities may be given by concentrations (dilute solutions), the surface excess may be obtained from the Gibbs Eq. (2)

$$\Gamma = -\frac{1}{nRT} \cdot \frac{\mathrm{d}\gamma}{\mathrm{d}\ln(c)} \tag{2}$$

where $n = 1$ for non-ionic surfactants, neutral molecules or ionic surfactants in the presence of excess electrolyte, and $n = 2$ for 1:1 ionic surfactants, assuming electrical neutrality of the interface [5]. Here Γ is the equilibrium surface excess, R the gas constant, T the Kelvin temperature and c the bulk surfactant concentration. The adsorption isotherm, Γ vs. c, can therefore be obtained by measuring the surface tension γ at various bulk surfactant concentrations. This can be done by a variety of techniques such as du Nouy ring, Wilhelmy plate or drop volume [1–4].

2.2. Adsorption isotherms obtained by neutron reflection

The application of neutron reflection (NR) to wet interfaces has been pioneered by Thomas and Penfold et al. [6–10]. The main advantages of NR are the ability to

contrast the surfactant layer by isotopic substitution, and the high accuracy to which Γ_{eq} can be obtained.

The reflectivity $R(Q)$ is measured as a function of momentum transfer, Q, where Q is a wave vector = $[(4\pi/\lambda) \sin \theta]$, λ is the wavelength of the neutrons (0.5–6.5 Å at ISIS), and θ the angle of incidence, which for wet interfaces is 1.5° using the reflectometers at ISIS in the UK. The neutron refractive index n of a component depends on its scattering length density ρ given by

$$\rho = \sum_i n_i b_i \tag{3}$$

b_i is the scattering length of nucleus i, with n_i its number density. Solutions of deuterated surfactant are made up in null reflecting water (nrw), a mixture of 8% D_2O in H_2O, where the scattering length density $\rho = 0$, and the refractive index $n = 1$, the same as for air. Due to the scattering length density being zero, there is no reflectivity from the nrw sub-phase and therefore the signal is from the surfactant monolayer. For these systems $R(Q)$ can be modelled [7,8] as a single uniform layer of surfactant of thickness τ and scattering length density of surfactant ρ_{surf}. The area per molecule, a_s, is given

$$a_s = \frac{\sum b}{\rho_{surf}\tau} \tag{4}$$

For neutral surfactants agreement between surface excesses measured by tensiometry and NR is generally very good [11–14]. An example of this is given in Fig. 3 for the non-ionic monododecyl octaethylene glycol ($C_{12}E_8$). There are no adjustable parameters in the treatment of the tensiometry data. However, with ionic surfactants, under certain conditions some discrepancies still remain [15–18], and this largely due to contamination of the surfactant by trace levels of divalent cations. These give rise to lowering the surface tension, and make interpretation of the γ-ln c curves difficult. This discrepancy can be described in terms of a modification in the prefactor of Eq. (2) used in the Gibbs isotherm, where α is the degree of surface dissociation [15].

$$\Gamma = \frac{1}{RT(2-\alpha)} \cdot \frac{d\gamma}{d\ln c} \tag{5}$$

This subject is still an ongoing debate in the literature, and most authors agree that this problem is far from trivial.

Due to there still being some controversy in values of Γ_{eq} obtained for anionic surfactants, the focus here will be on adsorption dynamics for non-ionic surfactants.

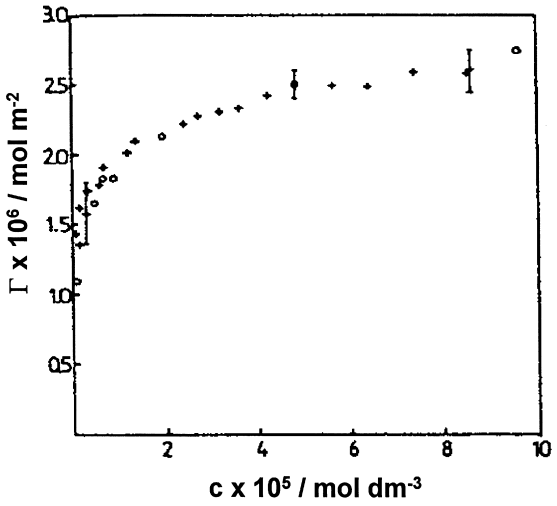

Fig. 3. Adsorption isotherm Of $C_{12}E_8$ as determined by neutron reflection (o) and from surface tension measurements (+). Taken from Thomas et al. [11], with permission from the American Chemical Society.

2.3. Empirical and theoretical adsorption isotherms

The main problem for interpreting DST is the application of an appropriate isotherm (e.g. [19,20]). The purpose of an adsorption isotherm is to relate the surfactant concentration in the bulk and the adsorbed amount at the interface. It is assumed that adsorption is monomolecular (a point borne out by NR studies). Apart from the Gibbs isotherm a number of other equations are also used, and these approaches are described now.

2.3.1. Henry isotherm

The simplest isotherm is

$$\Gamma = K_H c \tag{6}$$

where K_H is the *equilibrium adsorption constant*, which is an empirical measure of the surface activity of the surfactant [21].

This isotherm is only valid at low surface concentrations due to the assumption that there is no interaction between the adsorbed monomers and also there being no defined maximum value of Γ. The surface equation of state can be derived by applying the Gibbs equation, where $n = 1$ for neutral molecules and $n = 2$ for ionics

$$\pi = \gamma_0 - \gamma = nRT\Gamma \tag{7}$$

Here π defines the surface pressure and γ_0 the pure solvent surface tension.

2.3.2. Langmuir isotherm

This is the most commonly used non-linear isotherm [22–24]. It is based on a lattice-type model with the assumptions that:

1. every adsorption site on the lattice is equivalent;
2. the probability for adsorption at an empty site is independent of the occupancy of neighbouring sites; and
3. there are no interactions between the monomers in the lattice, and no intermolecular forces act between them.

This simple approach for describing adsorption is described next.

The rate of change of surface coverage due to adsorption is proportional to both the concentration of surfactant in solution, and the number of vacant sites available. The maximum number of sites available is Γ_∞.

$$\frac{d\Gamma}{dt} = k_a c \Gamma_\infty \left(1 - \frac{\Gamma}{\Gamma_\infty}\right) \tag{8}$$

The rate of change of Γ due to desorption is proportional to the number of adsorbed species:

$$\frac{d\Gamma}{dt} = k_d \Gamma \tag{9}$$

At equilibrium, these two rates are equal, and introducing the Langmuir equilibrium adsorption constant $K_L = k_{\text{ads}}/k_{\text{des}}$, results in the Langmuir isotherm,

$$\Gamma = \Gamma_\infty \left(\frac{K_L c}{1 + K_L c}\right) \tag{10}$$

There are two adjustable parameters in the above equation. The analogous surface equation of state for the Langmuir isotherm are the Szyszkowski [Eq. (11)] [25] and the Frumkin [Eq. (12)].

$$\pi = nRT\Gamma_\infty \ln(1 + K_L c) \tag{11}$$

$$\pi = -nRT\Gamma_\infty \ln\left(1 - \frac{\Gamma}{\Gamma_\infty}\right) \tag{12}$$

Deviations from the Langmuir isotherm may be attributed to the failure of the assumption of equivalent and independent sites. For example, intermolecular

forces act between the molecules at the interface, and these can be relatively small van der Waals or London dispersion forces, or larger forces due to electrostatic effects or hydrogen bonding. The enthalpy of adsorption often becomes less negative as Γ increases, suggesting the most energetically favourable sites are occupied first [26].

2.3.3. Frumkin isotherm

This approach builds on the Langmuir equation and it also accounts for solute–solvent interactions at a non-ideal surface [27]. It has been used in the study of many systems, and is most appropriate for non-ionic surfactants. Eq. (13) gives its usually quoted form:

$$c = \frac{1}{K_F} \cdot \frac{\Gamma}{\Gamma_\infty - \Gamma} \exp\left[-A\left(\frac{\Gamma}{\Gamma_\infty}\right)\right] \tag{13}$$

The three variables are the maximum adsorption Γ_∞, the Frumkin adsorption constant K_F and the constant A which depends on the non-ideality of the layer. If $A = 0$, then this equation reduces to the Langmuir isotherm [Eq. (10)]. The surface equation of state for the Frumkin isotherm is [28]:

$$\pi = -nRT\Gamma_\infty \ln\left(1 - \frac{\Gamma}{\Gamma_\infty}\right) - \frac{nRTA}{2}\Gamma_\infty\left(\frac{\Gamma}{\Gamma_\infty}\right)^2 \tag{14}$$

but due to the non-linearity of this equation no analytical expression for $\gamma(c)$ can be derived. However limiting or numerical solutions can be calculated.

2.3.4. Freundlich isotherm

This originated as an empirical equation, but can be theoretically derived by a model which considers the enthalpy of adsorption varying exponentially with surface coverage. It can be thought of as a summation of a distribution of Langmuir equations and its usual form for surfactant adsorption is given in Eq. (15) below:

$$\Gamma = kc^{1/n} \tag{15}$$

where k and n are both constants.

2.3.5. Volmer isotherm

This model accounts for non-ideal non-localised adsorption and also for the finite size of the molecules, with their interactions being calculated from statistical mechanics [29]. Its usual form is quoted below

$$c = K_v\left(\frac{\Gamma}{\Gamma_\infty - \Gamma}\right)\exp\left(\frac{\Gamma}{\Gamma_\infty - \Gamma}\right) \tag{16}$$

where K_v (units of concentration) is a constant.

This isotherm is not currently applied in the study of adsorption dynamics but is included in this discussion for completeness [30].

The above is a list of traditional isotherms used in solution chemistry, although there have been recent advancements to account for other physical properties of surfactants.

Borwankar et al. [31] extended the Frumkin isotherm to account for the electrical double layer, and Lunkenheimer et al. [32,33] have discussed new approaches in obtaining the surface equation of state.

Section 3 starts with the historical background to surfactant adsorption dynamics.

3. Surfactant adsorption dynamics: an historical background

In 1869 the first publication appeared suggesting the equilibrium surface tension was not achieved instantly. Dupré [34] presented evidence that tensions for fresh surfaces of soap solutions differed from their equilibrium value. This was also noted by Gibbs [35] in his theory of capillarity and by Rayleigh [36] who studied dynamics of soap solutions using the oscillating jet method. However, it was early into the 20th century before anyone proposed a mechanism of how surface tension changes with time. In 1907 Milner [37] measured the DST of sodium oleate and proposed that the formation of the interface was a result of surfactant diffusing from the bulk phase.

During the 1930s, there were many techniques investigated for measuring $\gamma(t)$ including Langmuir balances and electric surface potentials [38]. Adam and Shute [39,40] showed that adsorption processes at the liquid–gas interface could not be explained by a simple diffusion mechanism, as the diffusion process alone was too fast to explain the experimental data. They proposed monomers had to transfer through an adsorption barrier before they reached the interface. Goss [41] proposed the barrier was connected with the transfer of surface active ions through the electrical double layer formed by the adsorbed film.

Alexander [42] thought this barrier was connected with reorientation of surfactant molecules into the correct adsorption state before penetrating the interface. Others have also tried to quantitatively describe DST using a diffusion model; these include Bond and Puls [43], Ross [44], and Langmuir and Schaefer [45]. In 1944, Addison et al. [46–48] studied fast adsorption kinetics using various techniques and made attempts at estimating the magnitude of the adsorption barrier.

It was not until 1946 that a quantitative model for surfactant adsorption by a diffusion-only mechanism was published. This contribution by Ward and Tordai [49] is the backbone to most current DST modelling and is discussed in Section 4. During the 1950s it was thought that any minor impurities in the surfactant solutions, such as side products from the synthesis or excess reactants, were responsible for (or simulated) this adsorption barrier [50–53], and that DST with

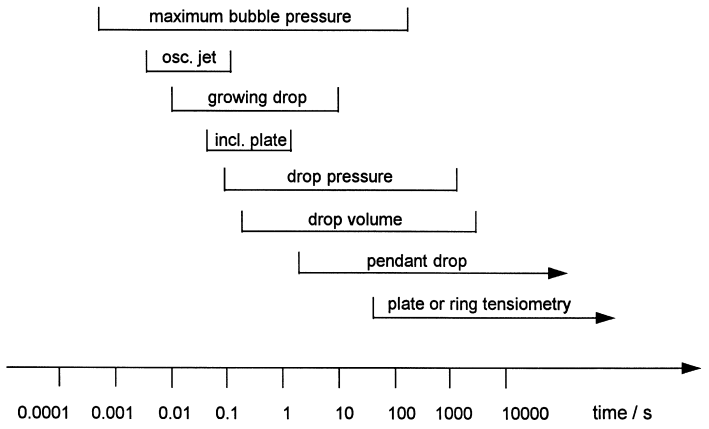

Fig. 4. Time windows for various DST techniques.

pure surfactants would be purely diffusion controlled. This, coupled with the lack of accurate and reproducible instrumentation and techniques, was responsible for the fall off of interest in the subject for the following few decades. There was a revival in DST studies in the 1990s due to the manufacture and availability of commercial set-ups of techniques such as maximum bubble pressure (MBP) [1,4,54] and drop volume [1,4] which made the field more accessible to new research groups. Recent books [1,2], and reviews [3,4], give details on the current techniques and commercial set-ups available for measuring both γ_{eq} and $\gamma(t)$. The plot in Fig. 4, taken from [1], shows the time windows over which dynamic surface tension measurements can be made using the techniques.

4. Mechanisms of surfactant adsorption

4.1. Diffusion-only mechanism

The most influential theoretical work was published by Ward and Tordai in 1946, and a summary follows.

4.1.1. The Ward and Tordai equation

The Ward and Tordai equation accounts for the diffusion of monomers from the bulk to the interface, and also the back diffusion into the bulk as the interface becomes more crowded. At the start of the process monomers from the subsurface adsorb directly, the assumption being that every molecule arriving at the interface is likely to arrive at an empty site, a reasonable postulate for the start of adsorption. However, as the surface becomes fuller, there is an increased probability that a monomer will arrive at an already occupied site. Back diffusion from the

subsurface to the bulk must then also be considered. If the subsurface concentration is known, then the diffusion of molecules from the subsurface to the bulk can also be treated with Fick's diffusion equations. The classic Ward and Tordai equation is given below in its usual quoted from:

$$\Gamma(t) = 2c_0\sqrt{\frac{Dt}{\pi}} - 2\sqrt{\frac{D}{\pi}}\int_0^{\sqrt{t}} c_s \mathrm{d}(\sqrt{t-\tau}) \tag{17}$$

where c_0 is the bulk surfactant concentration, D the monomer diffusion coefficient, c_s the concentration in the subsurface, $\pi = 3.142$ and τ is a dummy variable of integration. Owing to the convolution integral in the Ward and Tordai Eq. (17) to account for back diffusion, this equation cannot be solved.

In the following years, analytical solutions were proposed by Hansen [55,56] and Sutherland [57], although these can only be used under certain conditions, such as the dilute limit. It was not until recently that Miller, Fainerman and Makievski derived asymptotic solutions to the Ward and Tordai equation that could easily be applied to measured DST decays.

4.1.2. Asymptotic solutions to the Ward and Tordai equation

Limiting laws can be used to account for the DST when $\gamma(t)$ is close to that of the solvent γ_0, and for when it is close to the equilibrium value γ_{eq}. These asymptotic equations are given by Miller et al. [58] and their short derivations are given next.

4.1.2.1. Short time approximation, $t \to 0$. At the start of the adsorption process there will be no back diffusion. Neglecting this term from the Ward and Tordai Eq. (17) gives:

$$\Gamma(t) = 2c_0\sqrt{\frac{Dt}{\pi}} \tag{18}$$

An appropriate isotherm can be used to relate Γ and γ. At the start of adsorption when $\gamma \to \gamma_0$ the surfactant solution can be treated as dilute, so the linear Henry isotherm can be applied:

$$\gamma - \gamma_0 = -nRT\Gamma \tag{19}$$

where $n = 1$ for non-ionic surfactants, $n = 2$ for ionics. Substituting Eq. (19) into Eq. (18) gives

$$\gamma_{t\to 0} = \gamma_0 - 2nRTc_0\sqrt{\frac{Dt}{\pi}} \tag{20}$$

4.1.2.2. Long time approximation, $t \to \infty$. As $t \to \infty$ the subsurface concentration will get closer to the bulk concentration, and c_s can be factored outside the back diffusion integral in Eq. (17), with the integral now tending to unity as $t \to \infty$. Hence

$$\Delta c_{t\to\infty} = c_0 - c_s = \Gamma\sqrt{\frac{\pi}{4Dt}} \tag{21}$$

with the Gibbs equation

$$\mathrm{d}\gamma = -nRT\Gamma d\ln c \tag{22}$$

by taking the limit in Eq. (22) as $\Delta c \to 0$, the long time approximation can be stated as

$$\gamma_{t\to\infty} = \gamma_{\mathrm{eq}} + \frac{nRT\Gamma_{\mathrm{eq}}^2}{c}\sqrt{\frac{\pi}{4Dt}} \tag{23}$$

Both Eqs. (20) and (23) describe the adsorption process as a diffusion only mechanism due to being derived from the Ward and Tordai equation. Below, in Sections 5 and 6 these equations will be used to probe adsorption mechanisms.

4.2. Mixed diffusion-kinetic controlled adsorption: presence of an adsorption barrier

In this activated-diffusion mechanism, the monomers undergo diffusion from the bulk to the subsurface, obeying the same diffusion equations as for the diffusion only mechanism. However, once in the subsurface the monomer is not instantaneously adsorbed at the interface. It may have to do any of the following,

Overcome any potential energy barrier

In order to adsorb, a monomer has to do work against the increasing surface pressure π. When π is high it is unlikely that every molecule reaching the subsurface will have enough energy to adsorb at the interface. Only those molecules possessing an energy greater than a specified activation energy will be able to adsorb [59–68]. This is discussed in detail in Section 5.

Be in the correct orientation for adsorption

For the monomer to penetrate the surface film, it may have to adopt a certain configuration. This is particularly the case for very long chain surfactants, polymers and proteins [69–76] where the monomer may not adsorb if the chain is closely entangled within itself. In preference to rearranging itself in order to reach the adsorbed state, it may back diffuse into the bulk. Cho et al. [72] studied the dynamics of bovine serum albumin (BSA) by using a radiotracer method to measure $\Gamma(t)$.

They concluded that the evolution of $\Gamma(t)$ at short times was diffusion-controlled, but as adsorption continued there was an evolution of an electrostatic

energy barrier, which may partly be explained by the partial unfolding of the protein chain during adsorption. Ybert and di Meglio [74] also concluded that the initial stage of adsorption for BSA was diffusion-controlled by studies using pendant drop.

Pugh et al. [73,75] studied the DST of cellulose polymers using MBP and their results showed that there was a strong deviation from diffusion theory. They concluded that for the Ward and Tordai diffusion equation to be valid, the interface needs to be empty so that each molecule arriving at the surface can arrive at an empty site, and since this can only occur in the initial stages, the process overall is kinetically controlled and governed by an activation barrier.

Strike an 'empty site' in the interface

When present in the subsurface there has to be an 'empty site' in the interface above the monomer. Unlike the two factors above which were thermodynamically based, this is a statistical parameter.

The presence of micelles, and the time-scale for break-up, may hinder adsorption

Once the surfactant solution is above its CMC, the micelles present in the solution have a certain lifetime for break-up. If the micelles are stable entities with long lifetimes, the molecules in the micelles may not be available for adsorption [77–85].

In effect, the concentration of molecules diffusing to the interface will be equal to the CMC, regardless of the bulk concentration of surfactant, implying that the DST will not increase significantly above the CMC. This is discussed in detail in Section 6.

The term adsorption barrier can be used as a catch-all to incorporate any or all of the above factors that affect surfactant adsorption. This barrier will decrease the adsorption rate, and hence the transfer of monomer from the subsurface to the interface is the rate-determining step. If during adsorption none of the above need to be taken into account, then the adsorption barrier is in effect zero and the process is diffusion-only controlled.

Baret [59] made the first major attempt to account for this adsorption barrier and summarised the process as 'the number of solute molecules that adsorb at the interface is equal to the number of solute molecules which, having diffused from the bulk to the subsurface, cross the adsorption barrier'. He also concluded that the diffusion process is predominant at the start, but there is a switch over to mixed kinetics as maximum adsorption is attained.

An important contribution to the study of interfacial kinetic barriers has been given by Liggieri and Ravera [60,61]. Their model is based on the Ward and Tordai Eq. (17), but they introduce a renormalised diffusion coefficient which takes into account both the diffusion to the subsurface and then the crossing of the barrier. When considering the molecules in the subsurface, only those with energy larger than ε_a are adsorbed, whereas among the adsorbed molecules only those with

energy larger than ε_d are desorbed. The parameters ε_a and ε_d are activation energies of adsorption and desorption, respectively.

This renormalised diffusion coefficient D^* takes into account this activation barrier, and is related to the physical diffusion coefficient D by an Arrhenius-type relationship and is defined as:

$$D^* = D \exp(-\varepsilon_a/RT) \tag{24}$$

As $\varepsilon_a \to 0$, $D^* \to D$ and the process tends towards the diffusion-only controlled mechanism. Using D^*, this process can now be considered as a diffusion problem, which can be solved using Fick's equation with the new boundary condition

$$\frac{d\Gamma}{dt} = D^* \left(\frac{\delta c}{\delta x} \right)_{x=0} \tag{25}$$

giving a variation on the Ward and Tordai equation to account for a potential adsorption barrier:

$$\Gamma(t) = 2c_0 \sqrt{\frac{D_a t}{\pi}} - 2\sqrt{\frac{D_a}{\pi}} \int_0^{\sqrt{t}} c_s \mathrm{d}(\sqrt{t-\tau}) \tag{26}$$

where they define

$$D_a = \frac{D^{*2}}{D} = D \exp(-2\varepsilon_a/RT) \tag{27}$$

Further details on this approach to interfacial barriers can be found in Ravera et al. [60] and Liggieri et al. [61] and references therein.

4.3. Empirical modelling of DST: Rosen's approach

In a series of eight papers on DST by Rosen [86–93], DST curves could be modelled by an empirical equation, which at first seems to give little physical insight. However, it models experimental data well, and certain physical parameters can be indirectly inferred from it. It also gives a different approach to studying DST, as the simple mathematical equation can be built on to incorporate other physical models.

After examining a series of DST curves it can be seen that on a logarithmic time-scale, regardless of concentration or surfactant type, they all have essentially the same profile [86]. Typical curves are given in Figs. 6 and 7 in Section 5. Rosen divided this curve into four regions: (1) the induction region; (2) the rapid fall region; (3) the meso-equilibrium region; and (4) the equilibrium region.

Providing γ_0 and γ_{eq} are known for the surfactant solution, most dynamic surface tension data will fit the equation

$$\gamma(t) = \gamma_{eq} + \frac{\gamma_0 - \gamma_{eq}}{1 + (t/t^*)^n} \tag{28}$$

where n and t^* are constants, t^* having units of time, and n being dimensionless. These parameters can be obtained by reducing the DST data to an appropriate linear plot [86].

Eq. (28) can be manipulated to

$$\frac{\gamma_0 - \gamma_t}{\gamma_t - \gamma_{eq}} = \left(\frac{t}{t^*}\right)^n \tag{28a}$$

where the L.H.S. is the ratio of depression of surface pressure at time t to that remaining before equilibrium is attained. Rosen defined the induction region to end when this ratio equals $1/10$ and for the rapid fall region to end when the ratio equals 10.

The two parameters n and t^* can give insight into the characteristics of the surfactant, such as concentration of the solution, surfactant type, hydrophobic nature, diffusion coefficients and area per molecule at the air–water interface by applying this equation to experimental data. This empirical approach has been built on by Fillipov and Fillipova [94–97] in their theoretical consideration of DST, and also by Svitova et. al. [98] in their studies of siloxane surfactants.

The following sections discuss experimental DST measurements in relation to these models.

5. Dynamic surface tensions of monomeric non-ionic surfactant solutions

The experimental part of this review begins with a discussion on the DST of monomeric neutral surfactants. Two independent studies have recently been carried out by Lin et al. [63,64] and Eastoe et al. [66,67], both groups arrive at similar conclusions: a mixed mechanism operates at higher surfactant concentrations.

5.1. DST as a function of concentration

Lin et al. [62,99] studied decanol solutions and concluded that the cohesive forces between the adsorbed molecules play an important role in the adsorption kinetics. These long chain alcohols with small polar groups are subject to strong, attractive van der Waals forces when the interface becomes saturated. It was suggested that these cohesive forces contribute to the observed energy barrier.

To quantitatively account for the adsorption rate, and incorporate an activation barrier, they used the Langmuir isotherm. Hence, the rate of adsorption is proportional to the subsurface concentration c_s, and the number of interfacial sites

that are available for adsorption $(1 - \Gamma/\Gamma_{max},)$. The desorption rate is proportional to the surface coverage Γ. The overall adsorption rate may be written:

$$\frac{d\Gamma}{dt} = [\beta \exp(-E_a/RT)].c_s(\Gamma_\infty - \Gamma) - [\alpha \exp(-E_d/RT)]\Gamma \quad (29)$$

where β, α, $E_a(\Gamma)$ and $E_d(\Gamma)$ are pre-exponential factors and activation energies for adsorption and desorption with the adsorption rate constant being defined as $\beta \exp(-E_a^0/RT)$. Γ_∞ is the maximum number of available sites.

To account for the activation energy increasing with surface pressure, the activation energies are a function of Γ:

$$E_a = E_a^0 + \nu_a \Gamma^n \quad (29a)$$

$$E_d = E_d^0 + \nu_d \Gamma^n \quad (29b)$$

where E_a^0, E_d^0, ν_a and ν_d are all constants.

At equilibrium when $d\Gamma/dt = 0$, the equilibrium isotherm is

$$\frac{\Gamma}{\Gamma_\infty} = x = \frac{c}{c + a\exp(kx^n)} \quad (30)$$

where $k = (\nu_a - \nu_d)\Gamma_{max}^n/RT$ and $a = (\alpha/\beta)\exp(E_a^0 - E_d^0)/RT$. When $n = 1$ the Frumkin isotherm results, and when $\nu_a = \nu_d = k = 0$ Eq. (30) reduces to the Langmuir isotherm. From pendant drop experiments on decanol solutions, it was concluded that the activation barrier plays a greater role at the tail end of the process, as it is only at these extended times that the interfacial concentration is high enough for the interactions to be important.

Lin et al. [63,64] have also performed studies on two non-ionic polyoxyethylene alcohols, $C_{12}E_8$ and $C_{10}E_8$ and analysed the DST data in a similar way. For both these surfactants they concluded that the controlling mechanism for mass transfer can change as a function of bulk concentration from diffusion to mixed kinetic-diffusion control. The DST curves for $C_{10}E_8$ solutions, with a wide range of pre-CMC concentrations, are given in Fig. 5a. Fig. 5b shows how the apparent (or effective) diffusion coefficient of the molecules, D_{eff}, decreases as the concentration is increased. This indicates that the adsorption of $C_{10}E_8$ molecules onto a clean air–water interface is not purely diffusion controlled. These values were obtained by applying different adsorption isotherms, further information can be found elsewhere [62–64,99]. The Frumkin isotherm gave a better agreement to their measured data than the Langmuir equation, indicating that the intermolecular interactions between the adsorbed molecules are significant.

From examining these DST decays (Fig. 5a), and how D_{eff} changes with concentration (Fig. 5b), this evidence would suggest a diffusion-controlled mechanism at dilute bulk concentrations, where the equilibrium surface coverage is low, and mixed kinetic-diffusion control as the bulk concentration becomes higher and the equilibrium surface coverage is increased. In comparing their theoretical profile

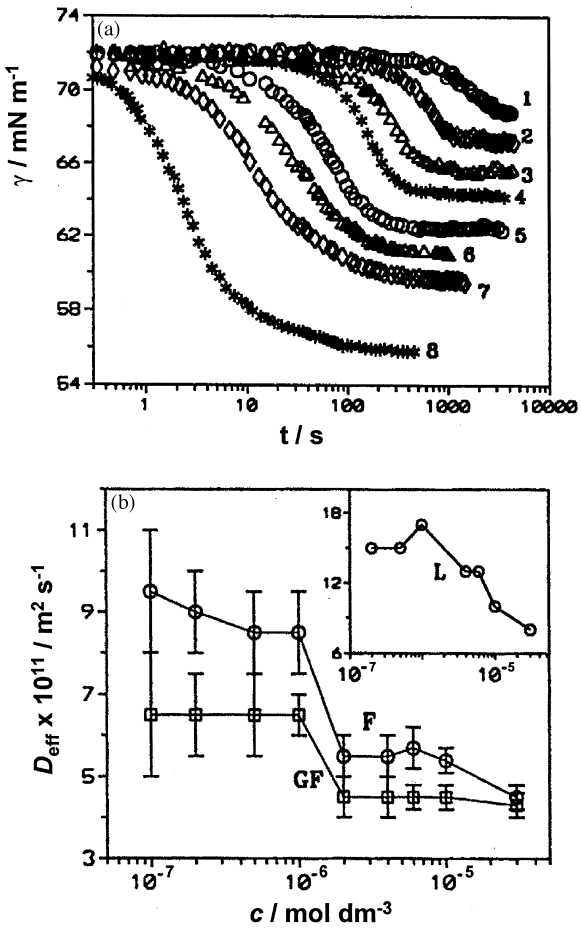

Fig. 5. (a) DST of $C_{10}E_8$ solutions according to Lin et al. Reproduced from Lin et al. [62]. Concentration = (1) 0.20; (2) 0.50; (3) 1.0 (4) 2.0; (5) 4.0; (6) 6.0; (7) 10.0; (8) 30.0 [$\times 10^6$/mol dm^{-3}]. (b) Values of the effective diffusion coefficient D_{eff} from the DST data, and the model predictions from the Frumkin, generalised Frumkin and Langmuir isotherms as a function of concentration. Reproduced from Lin et al. [62], with permission from the American Chemical Society.

[Eqs. (29) and (30)] and experimental DST curves they concluded that the adsorption/desorption process varies significantly with surface coverage rather than purely bulk concentration and the adsorption becomes more difficult as the surface becomes more crowded.

This behaviour has also been observed by Eastoe et al. in studies of similar non-ionics [66,67]. DST measurements by maximum bubble pressure (LAUDA MPT1 [1,4,54,100]) were made on solutions of $C_{10}E_4$ and $C_{10}E_5$ below the CMC and example profiles of $C_{10}E_4$ are shown in Fig. 6. Here, t_{eff}, the effective lifetime of the bubble has been previously described in [1,54], and the equipment is

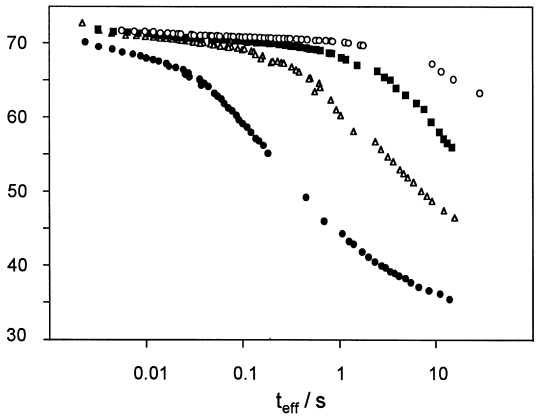

Fig. 6. Dynamic surface tensions of monomeric $C_{10}E_4$ solutions. Concentration $\times 10^3$/mol dm^{-3}: 0.50 (●), 0.20 (△), 0.10 (■), 0.05 (○). CMC = 0.61×10^{-3} mol dm^{-3}.

carefully calibrated [66]. Using the approach of Miller et al. (Section 4.1.2), analysis showed that the initial stages of adsorption were described well by a diffusion only approach when the interface is empty. However, towards the end of adsorption it was observed that the DST decay was not described well by a diffusion mechanism, with the measured tension being consistently higher than that predicted by the long time diffusion [Eq. (23)]. In this analysis, the measured value of Γ_{eq} had been obtained from tensiometric data, and as discussed in Section 2 it is expected that this value would be in good agreement with neutron reflectivity measurements, so a high accuracy on Γ is expected.

The monomer diffusion coefficient D was obtained by pulsed field gradient spin echo NMR measurements (PFGSE NMR) as described by Griffiths et al. [101].

Fig. 7 shows the data, and predictions, for a $C_{10}E_4$ solution at 5×10^{-4} mol dm^{-3} (0.8 × CMC). After 30 ms the tension drop from γ_0 is approximately 6 mN m^{-1}, and Eq. (20) clearly describes these early stages of the decay well. Similar agreement between the initial parts of the decays and Eq. (20) was found for other concentrations of $C_{10}E_4$ and $C_{10}E_5$ studied. It can be seen in Fig. 7 that for this example the prediction fails above 30 ms.

Turning now to the end of the decay for this sample, at $t > 30$ ms there is poor agreement with Eq. (23). The diffusion-controlled adsorption model consistently predicts a lower tension than is measured: at 1 s the difference is some 12 mN m^{-1}, and at 10 s, where from Eq. (23) the tension should be essentially γ_{eq}, it is approximately 5 mN m^{-1}. Similar discrepancies between the long time DST data and Eq. (23) were seen for $C_{10}E_5$ below the CMC. This behaviour is entirely consistent with the presence of a weak adsorption barrier. Attempts at evaluating the barrier were made by measuring the DST as a function of temperature. This enabled the activation barrier to be estimated using the approach of Liggieri et al. [60,61].

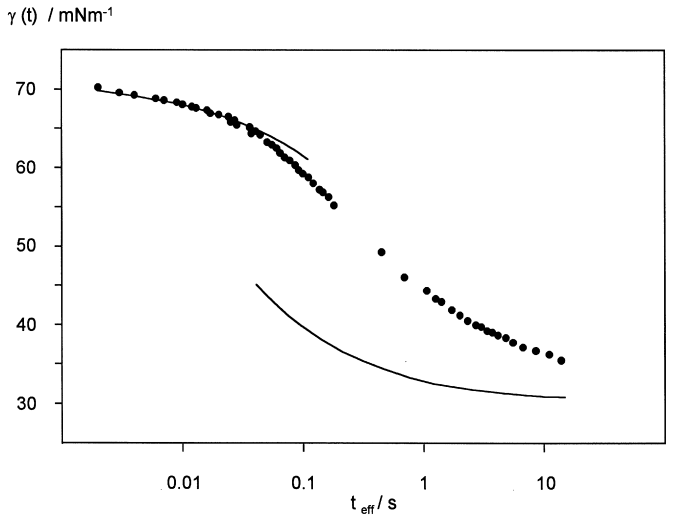

Fig. 7. DST for $C_{10}E_4$ below the CMC at 5×10^{-4} mol dm^{-3} (●). Lines are calculations using Eqs. (20) and (23) at long and short times, respectively. With permission from Academic Press.

5.2. DST as a function of temperature

The type, and quality, of surfactant selected for DST experiments is an important factor. As previously mentioned, the presence of any impurities in the surfactant may well be responsible for any observed adsorption barrier. It is also essential that the adsorption dynamics of simple non-ionics is well understood, before the more complex ionic compounds are investigated.

In addition, certain non-ionics are ideal for initial studies as their equilibrium adsorption properties are well documented. This is the case for the di-chained non-ionic glucamide surfactant, $(C_6H_{13})_2C[CH_2NHCO(CHOH)_4CH_2OH]_2$ (di(C6-Glu)) [101–105], and therefore this surfactant was chosen for dynamic study. The DSTs were measured as a function of temperature in order to be tested by the Arrhenius-type expression suggested by Liggeiri et al. [Eq. (24)]. Although it is generally accepted that the initial adsorption, where the surface coverage is low, is purely diffusion controlled there is still some controversy about the underlying mechanism closer to equilibrium. These experiments show that for this monomeric non-ionic surfactant, the final stages of the $\gamma(t)$ decay as a function of temperature are consistent with Arrhenius-like behaviour, and an activation-diffusion controlled adsorption mechanism.

5.2.1. Equilibrium properties of di-(C6-Glu)

The glucamide surfactant was ideal for this temperature study due to there being no cloud point up to 90°C. In addition, extensive du Nouy measurements, over the range 10–50°C, show that both the CMC and the maximum adsorbed amount Γ_{max}

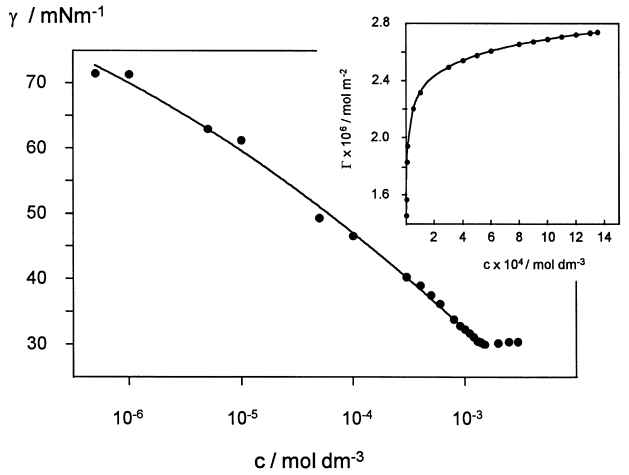

Fig. 8. Equilibrium surface tension γ vs. concentration c for di-(C6-Glu). The fit is a quadratic to the pre-CMC data. The inset shows the Γ vs. c isotherm derived from the Gibbs equation. With permission from Academic Press.

are essentially constant: they may be taken as $(1.35 \pm 0.05) \times 10^{-3}$ mol dm^{-3} and $(2.75 \pm 0.25) \times 10^{-6}$ mol m^{-2} [102–105]. The γ vs. c curve for di-(C6-Glu) is given in Fig. 8, and the clear break in the plot defining the CMC gives evidence of high surfactant purity. The pre-CMC data fits to a quadratic, and at each concentration tangents to these fitted functions were used to obtain the surface excesses via the Gibbs isotherm. The inset to the figure shows the Γ vs. c isotherm.

The isotherms obtained by both tensiometry and neutron reflectivity [100,104] are in good agreement and show that Γ is effectively constant down to CMC/10. All of these properties make di-(C6-Glu) an ideal surfactant for studying the effects of temperature on DST. The monomer self diffusion coefficient, D, has been measured below the CMC at 8.0×10^{-4} mol dm^{-3} and a temperature of 25°C using PFGSE-NMR [67,101], and this gave $D = 2.70 \times 10^{-10}$ m^2 s^{-1}.

5.2.2. Dynamic surface tension of di-(C6-Glu)

For non-ionics Eq. (23) is (see Section 2)

$$\gamma(t)_{t\to\infty} = \gamma_{eq} + \frac{RT\Gamma^2}{2c}\left(\frac{\pi}{Dt}\right)^{1/2} \tag{31}$$

where γ_{eq}, c, Γ and D represent the equilibrium tension, bulk concentration, surface excess and monomer diffusion co-efficient of the surfactant. If the adsorption were purely diffusion-controlled, then this equation should account reasonably well for the end of the tension decays, since a rigorous analysis of this equation indicates that this approach is valid for investigating the adsorption mechanism [100,106].

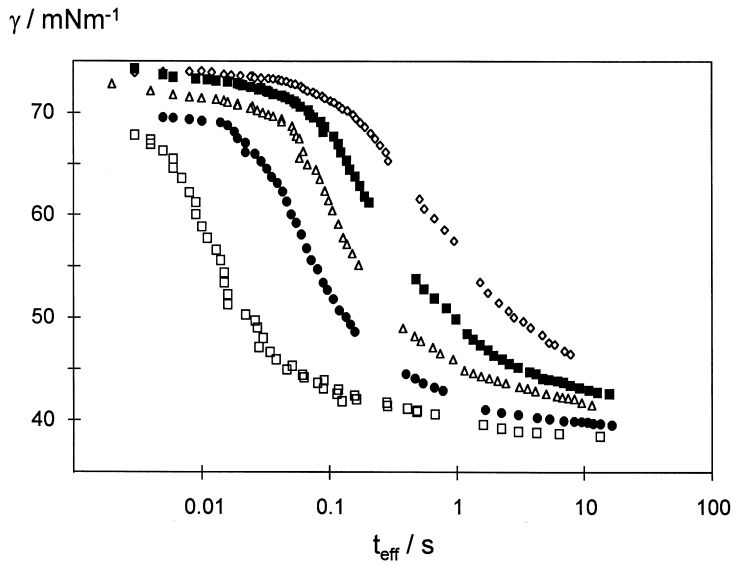

Fig. 9. Dynamic surface tensions for solutions of di-(C6-Glu), below the CMC at 5×10^{-4} mol dm^{-3}, as a function of temperature. T in °C: 10.0 (◇); 20.0 (■); 30.0 (△); 40.0 (●); 50.0 (□). With permission from the American Chemical Society.

Fig. 9 shows the DST of di-(C6-Glu) as a function of temperature measured by MBP, and it is clear that increasing T gives rise to a faster decay. The equilibrium surface tension was measured as a function of T by du Nouy tensiometry, with γ_{eq} decreasing from 41.0 mN m^{-1} at 10°C to 36.9 mN m^{-1} at 50°C. Between 20 and 50°C the DST decays were therefore essentially complete, with the final points close to the du Nouy values. At 20°C the last DST measurement was 1.8 mN m^{-1} above γ_{eq} and at 50°C this difference was 0.7 mN m^{-1}.

The difference in γ_0 (the surface tension of the solvent) at the start of the decay is consistent with the effect of temperature on the surface tension of water.

In order to test equation 31 the DST data are plotted as a function of $t^{-1/2}$ in Fig. 10. The data are linear at long times, suggesting a diffusion-type process. The lines are least squares fits for $t > 0.25$ s (i.e. $t^{-1/2} < 2$), with the intercepts equal to the equilibrium tensions measured by the du Nouy ring. The gradients of these fitted lines are given in Table 1, along with values for the effective diffusion coefficients, D_{eff}, calculated from the slopes using

$$D_{\text{eff}} = \left(\frac{RT\Gamma^2 \pi^{1/2}}{2c.\text{gradient}} \right)^2 \tag{31a}$$

which can be obtained by rearranging Eq. (31). As seen, D_{eff} increases by almost

Table 1
Gradients of DST decays and diffusion coefficients as a function of temperature for di-(C6-Glu) solutions at 5×10^{-4} mol dm^{-3} (D measured at 25°C, by PFGSE-NMR is 2.70×10^{-10} m^2 s^{-1})

T (°C)	Gradient (mN m^{-1}s$^{1/2}$)	$D_{eff} \times 10^{10}$ (m^2 s^{-1})	$D \times 10^{10}$ (m^2 s^{-1})	D_{eff}/D
10	15.1	0.032	1.74	0.018
20	9.6	0.086	2.24	0.038
30	6.6	0.20	3.04	0.068
40	3.7	0.66	3.93	0.168
50	2.0	2.32	4.83	0.480

two orders of magnitude on increasing the temperature from 10 to 50°C indicating that temperature is an important parameter governing DST.

The monomer self-diffusion coefficient, D (2.70×10^{-10} m^2 s^{-1} at 25°C), obtained from PFGSE-NMR measurements was used to estimate D values at the other temperatures. Both temperature T and viscosity η of the solution will have an effect on D, and each of these will be considered in turn. Firstly, giving attention to temperature, assuming a Stokes–Einstein-like relationship holds for the solutions studied here, then $D\alpha T$. Viscosity, has a larger effect on D, as its relationship is exponential with temperature [26].

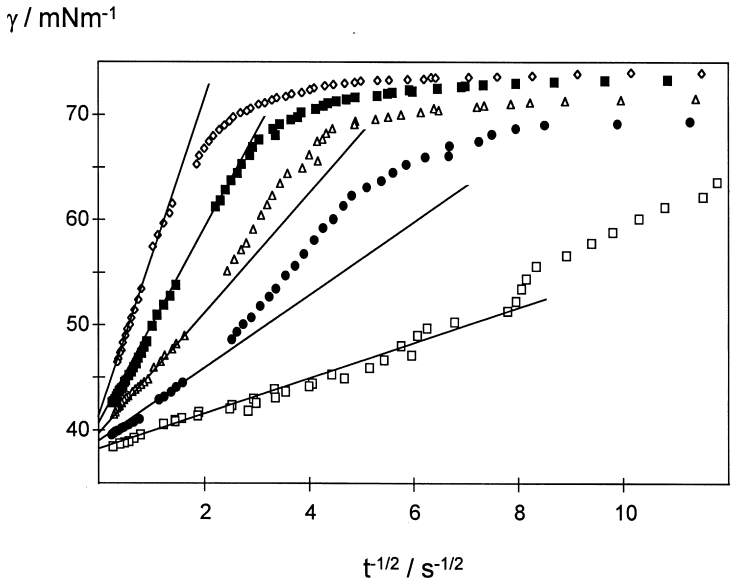

Fig. 10. DST data of Fig. 9 plotted against $t^{-1/2}$ in line with Eq. (31). Lines are least squares fits with $\gamma \rightarrow \gamma_{eq}$ as $t \rightarrow \infty$. Symbols are the same temperatures as Fig. 9. With permission from the American Chemical Society.

Combining the two influences of temperature and viscosity, the estimated D values are reported in Table 1 along with ratios D_{eff}/D.

The increase in the value of D over the temperature range is small compared to the increase in D_{eff}. For example at 10°C the value of D is 36% of that at 50°C, whereas for D_{eff} this value is 1.4%. At 10°C the ratio D_{eff}/D is 0.018 indicating that the measured tension is substantially higher than that predicted by Eq. (32), and that there is a significant adsorption barrier. At 50°C the ratio D_{eff}/D is relatively close to 1, suggesting a near diffusion-controlled adsorption at this temperature.

Alternatively, the Hansen equation [55]

$$\gamma(t)_{t\to\infty} = \gamma_{\text{eq}} + \frac{RT\Gamma^2}{c}\left(\frac{1}{\pi Dt}\right)^{1/2} \tag{32}$$

could also be used to analyse the long-time DST, and Miller et al. have recently made a comparison of Eqs. (31) and (32) for this purpose [106]. The diffusion coefficients derived from Eq. (3) are lower than those in Table 1 by a factor of $\pi^2/4$ (≈ 2.47). However, this does not change the conclusion that only at 50°C is the DST close to diffusion-controlled.

Fig. 11 shows the measured and predicted tensions for the $\gamma(t)$ curves at 10 and 50°C. At 50°C Eq. (32) appears to account for the measurements reasonably well from 0.01 s onward. At 10°C the calculated tension is too low, and it is clear that temperature has a more important effect on the measured DSTs than is predicted by the diffusion-only theory, even taking into account the combined effect of T and $D(T,\eta)$ in Eq. (31).

5.2.3. Activated-diffusion mechanism: calculation of the adsorption barrier

Liggeri et al. [60,61] suggested that if the mechanism was mixed diffusion–activation, then D_{eff} should obey an Arrhenius-like equation [Eqs. (24) and (27)]. Their calculations show that raising E_a can cause a significant decrease in the adsorption $\Gamma(t)$, especially in the long time limit. Their calculations for $\Gamma(t)$ at long times show that only relatively small barriers can have a significant effect, and for any given time raising E_a will increase γ. For example at 10 s, with a surfactant MW 600, the predicted adsorptions Γ for E_a 1.1 RT and 3.2 RT are a factor of 5 and 10 lower as compared to that for the purely diffusion-controlled model. However, at the start of the adsorption and short times, $\gamma(t)$ data cannot be used to clearly discriminate between diffusion-only and mixed mechanisms. A number of alternative theoretical approaches have also been proposed to account for the effects of adsorption barriers [94–98,106] and although these treatments have met with some success they do not appear to be generally applicable to these experimental results.

Alternatively this activation barrier may be expressed as

$$D_{\text{eff}} = D\exp(-\Delta G/RT) \tag{33}$$

where ΔG represents the free energy change for the formation of an activated

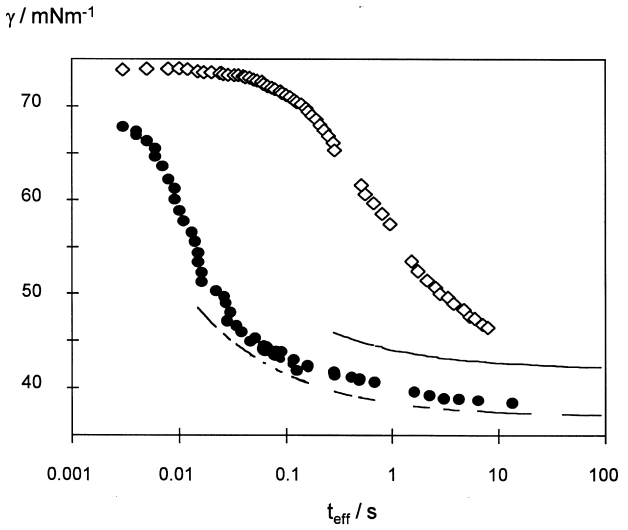

Fig. 11. DST of a 5×10^{-4} mol dm^{-3} di-(C6-Glu) solution at 10°C (◇) and 50°C (●). The filled line and the broken line are from calculations described in the text at 10 and 50°C, respectively. With permission from the American Chemical Society

state. The separate entropy and enthalpy contributions, ΔS and ΔH, can be introduced and then

$$D_{\text{eff}} = D \exp(\Delta S/R) \exp(-\Delta H/RT) \tag{33a}$$

or

$$\ln\left(\frac{D_{\text{eff}}}{D}\right) = \frac{\Delta S}{R} - \frac{\Delta H}{RT} \tag{33b}$$

Of course it must be assumed that the activation parameters do not depend significantly on temperature, at least over the range studied [107].

For the di-(C6-Glu) Fig. 12 shows a plot of $\ln(D_{\text{eff}}/D)$ vs $1/T$, in line with Eq. (33b). The apparent enthalpy and entropy changes, obtained from the equation of the line, are $\Delta H = +62 \pm 1$ kJ mol^{-1} and $\Delta S = +180 \pm 5$ JK^{-1} mol^{-1}. In Fig. 13 values for $-\ln(D_{\text{eff}}/D)$ are shown as a function of concentration, but determined at a fixed temperature of 25°C for various non-ionic surfactants (see key). Using Eq. (33) the mean value of ΔG is $+7.5$ kJ mol^{-1}, and this is consistent with the values of ΔH and ΔS determined separately in the temperature variation experiments ($62 - 54 = 8$ kJ mol^{-1}). The values for the thermodynamic parameters suggest both temperature and concentration variation experiments can be reconciled by assuming an activated state forms prior to adsorption. The specific nature of this state is unclear, however some insight may be gained by comparing the activation parameters with values for ΔH_{ads} and ΔS_{ads} which relate to

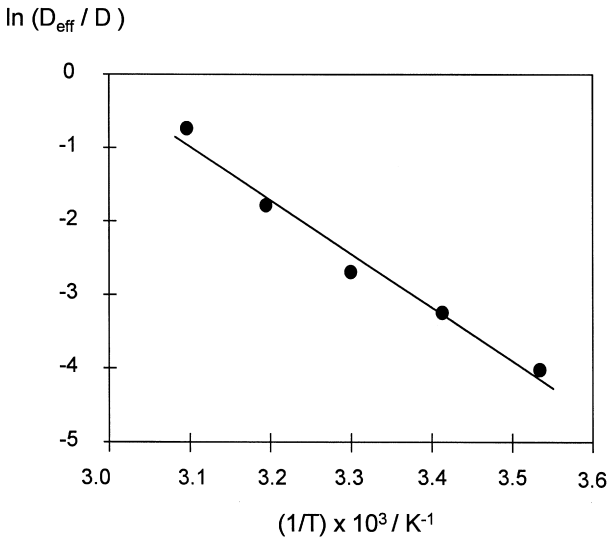

Fig. 12. Arrhenius-type plot for a di-(C6-Glu) solution at 5×10^{-4} mol dm^{-3}. The fitted line gives $\Delta H = +62$ kJ mol^{-1}. With permission from the American Chemical Society.

adsorption into the film at equilibrium [93]. For C_{12} ethoxylated sulfonates and sulfates Rosen et al. found ΔH_{ads} ranging from $+2.4$ to -12.5 kJ mol^{-1}, with ΔS_{ads} between about 80 and 110 JK^{-1} mol^{-1} [93]. (Although they are anionic these surfactants contain EO groups, and bear a close resemblance to the non-ionics discussed here).

The positive entropy change for the formation of the activated and equilibrium states is consistent with the hydrophobic effect, and a 'release of ordered water molecules'. The formation of the activated state is endothermic, whereas for the equilibrium state ΔH_{ads} is generally exothermic. These differences may reflect the energetic requirement for molecules attain sufficient energy to penetrate the film.

Miller et al. have also seen a similar dependence of DST with temperature [100]. For a pre-CMC solution of Triton X-100 at 1.55×10^{-4} mol dm^{-3} it was observed that the gradient $d\gamma/dt^{-1/2}$ also decreases with temperature. For example at 30°C the slope was 17 mN m^{-1} s$^{1/2}$ whereas at 70°C it was 8 mN m^{-1} s$^{1/2}$. Using estimated values for $D \cong 2.6 \times 10^{-10}$ m^2 s^{-1} and $\Gamma = 2.65 \times 10^{-6}$ mol m^{-2} this is consistent with an enthalpy of activation of ~ 40 kJ mol^{-1} for this surfactant. A comparison of this with the value obtained here for di-(C6-Glu) is not appropriate as Triton X-100 is only a technical grade surfactant and not as well suited to a temperature variation study.

6. Dynamic surface tensions of micellar non-ionic surfactant solutions

It has been proposed that the presence of micelles may also play a role in DST.

If the overall micellar lifetime τ_2 [108–110] is longer than the time taken for $\gamma(t)$ to reach γ_{eq} then the micellised surfactant may not be available for adsorption, and hence the DST will decay more slowly.

Adsorption of monomers results in a concentration gradient at the subsurface. This gradient will return to equilibrium, on one hand by the usual diffusion of monomers in the bulk, and also by the break up of micelles in the subsurface region. It is reasonable that the aggregation number, which is linked to τ_2, may influence the adsorption dynamics. Joos et al. [79] and later Fainerman et al. [81–84] turned this argument around to obtain estimates for rate constants k_{mic} $(= 1/\tau_2)$ from DST measurements on micellar solutions.

This study [79] yielded the following relationship between k_{mic} and $\gamma(t)$:

$$k_{mic} = \frac{1}{\pi}\left[\frac{(d\gamma/dt^{-1/2})_{t\to\infty,\ c=CMC}}{(d\gamma/dt^{-1})_{t\to\infty,\ c>CMC}}\right]^2 \tag{34}$$

and hence [82,83]

$$\gamma(t)_{t\to\infty} = \gamma_{eq} + \frac{nRT\Gamma^2}{2c_0 t}\sqrt{\frac{\pi}{Dk_{mic}}} \tag{35}$$

Fainerman et al. suggest that Eq. (35) should be used rather than Eq. (23) above the CMC. This relationship, and the theory of micellar influences on DST, has been tested with non-ionic surfactants.

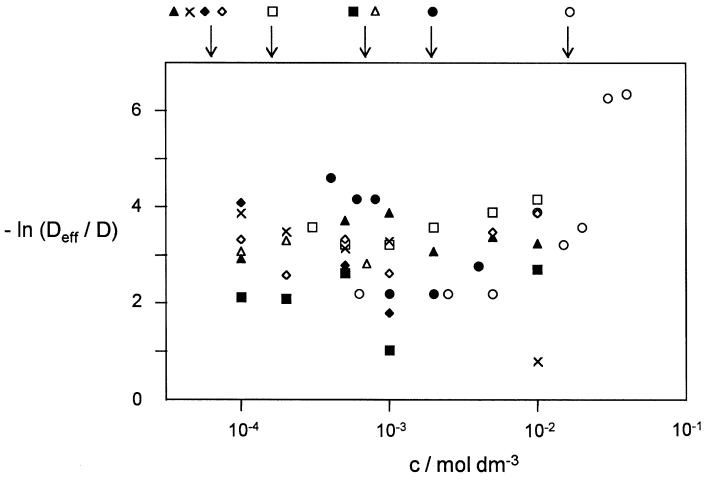

Fig. 13. Values of $-\ln(D_{eff}/D)$ vs. concentration c for C_nE_m and glucamide surfactants. Arrows indicate the CMCs. $C_{10}E_4$ (■), $C_{10}E_5$ (△), $C_{12}E_5$ ( ), $C_{12}E_6$ (◇), $C_{12}E_7$ (◆), $C_{12}E_8$ (×), di-(C5-Glu) (○), di-(C6-Glu) (●), di-(C7-Glu) (□). With permission from Academic Press.

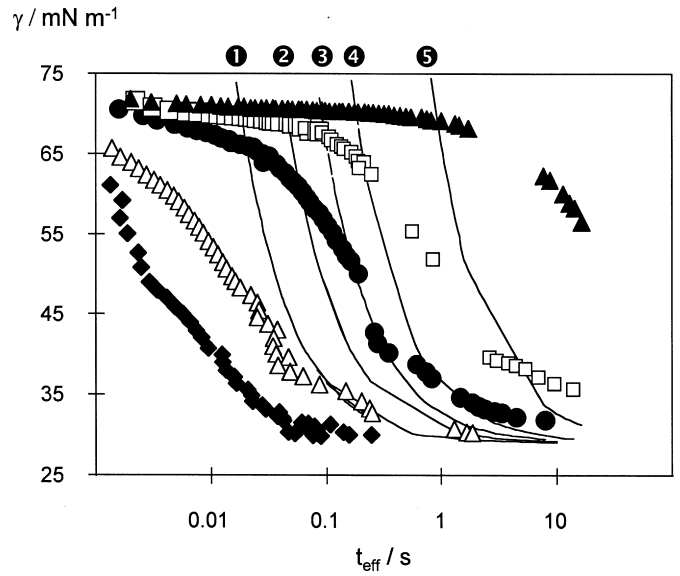

Fig. 14. DST of micellar solutions of $C_{12}E_5$ (shape markers) and calculations accounting for micellar kinetics using Fainerman's Eq. (35) (numbers in circles). Concentration × CMC: 100 (♦) and (♦); 40 (△) and (△); 20 (●) and (●); 10 (□) and (□); 2 ( ) and (△).

6.1. The effect of micelles on the DST of non-ionic surfactants

DST measurements using MBP have been carried out on a variety of C_nE_m surfactants (n = 8, 10, 12; m = 4, 5, 6, 7, 8) and glucamide surfactants both above and below their CMCs (cloud and Krafft points were avoided) [66,105,111]. At the beginning of adsorption all the surfactants and concentrations were consistent with a diffusion-only mechanism.

At the end of adsorption, as similarly seen for monomeric $C_{10}E_4$ and $C_{10}E_5$ solutions, there was evidence of an adsorption barrier. The effective diffusion coefficient D_{eff} obtained by applying Miller's diffusion equations to MBP data was somewhat less than the physically measured value of the diffusion coefficient D, measured say by PFGSE-NMR. What is somewhat surprising, however, is that broadly speaking, the ratio D_{eff}/D appears independent of both surfactant and concentration, both below and above the CMC. Fig. 13 demonstrates this, and individual CMCs are marked.

This conclusion does not agree with theoretical predictions of Joos et al. and Fainermann et al. descried previously. In order to test out these ideas k_{mic} values were measured for some C_nE_m surfactants using absorbance stopped-flow [111]. For certain compounds the values of k_{mic} were in good agreement with those of Tiberg et al. [112], who carried out similar measurements using ellipsometry. Both these independent methods gave values of k_{mic} for $C_{12}E_5$ and $C_{12}E_6$ as 0.10 s^{-1} and 0.17 s^{-1}, respectively. Furthermore, Tiberg et al. concluded that these lifetimes

are in agreement with the generally accepted model of Aniansson and Wall [108–110].

Using $C_{12}E_5$ as an example, DST decays suggested by Eq. (35) were synthesised using the measured values of k_{mic}, D and Γ. These curves were compared to the experimental data [111], and examples are shown in Fig. 14. At low micellar concentrations the predicted tensions are too low, and at higher concentrations they are too high. A similar treatment was applied to $C_{12}E_6$, at a concentration of 5×10^{-4} mol dm^{-3} ($\sim 6 \times$ CMC) and this is shown in Fig. 15. The calculated lines on the figure represent the predicted tensions at various example values of k_{mic}, including the experimentally measured value of $k_{mic} \sim 0.17$ s^{-1}. This was typical for the other concentrations and surfactants studied, suggesting the effects of micelles on the DSTs are minimal, at least under the conditions studied so far.

It would appear that micelle dissociation may only be important when the concentration of monomer in the subsurface is limiting or when the value for k_{mic} is small. These conditions occur with very hydrophobic surfactants where the CMCs are low, and also ones which have long micellar lifetimes.

It was seen that even for the most hydrophobic surfactant studied, $C_{12}E_5$, where CMC $\sim 5 \times 10^{-5}$ mol dm^{-3} and $\tau_{mic} \sim 10$ s, the DST decays were best described by incorporating an activation barrier into Miller's diffusion equations [Eqs. (20) and (23)]. From these results it can be concluded that there are no special considerations needed for surfactant solutions above the CMC, at least for the surfactants and concentration range studied here.

An explanation for this has been proposed by Johner and Joanny [113] who were interested in the dynamic adsorption of A–B block copolymers, which also micel-

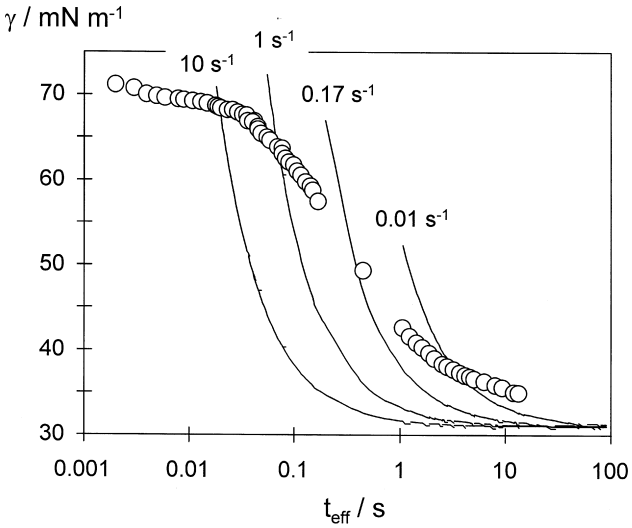

Fig. 15. Markers show measured DST decay of $C_{12}E_6$ at $6 \times$ CMC. Lines give decays predicted by Eq. (35) at various k_{mic} values.

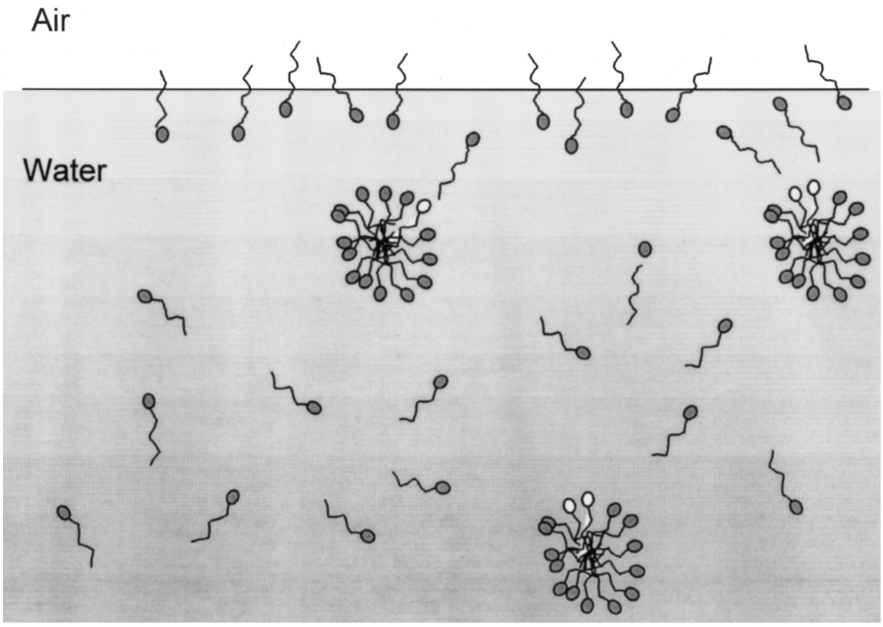

Fig. 16. Schematic showing how micelles in the subsurface can leak fresh monomer on the microsecond time-scale. These free monomers may then be available for adsorption.

lise. They suggested that the relaxation time, τ_1, for the release of monomer from the micelle into the bulk is the important process to be considered, rather than the longer time-scale of complete micellar break-down, τ_2. Micelles which are in the subsurface can 'leak', thereby releasing one or two molecules, and then leave this region to be replaced by another micelle that can similarly supply more monomer. A schematic demonstrating this is shown in Fig. 16. Since this characteristic monomer lifetime, τ_1, is typically 10^{-6} to 10^{-4} s [108–110], the micelles can be treated as a sink of monomers which are readily available for adsorption over the timescale of the DST process studied here, and therefore the micelles will not limit adsorption. It can be concluded that the shorter relaxation time τ_1 is important for supplying fresh monomer from the micelle to the interface, rather than assuming that the monomer is tightly bound and only released over the longer relaxation time, τ_2.

7. DST studies of anionic surfactants

The main problem to be overcome in any study of anionic surfactants is that of purity. As well as surface active impurities arising from unreacted intermediates and hydrolysis unreacted reagents, it has also been realised that trace divalent ions can also have an important effect on the equilibrium $\gamma - \ln c$ curve. However,

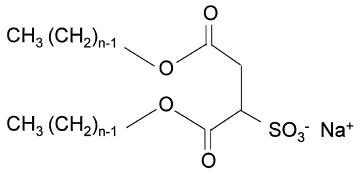

Fig. 17. General structure of diCnSS surfactants.

Miller et al. have studied *n*-alkylsulfates with chain lengths $C_{10} \rightarrow C_{16}$[58]. For most compounds studied, the start of the DSTs were consistent with diffusion control. Although, especially with the short chain surfactants, there was some evidence for an adsorption barrier, although this may have been due to impurities. The authors indicated that over long times the data are described by a diffusion-controlled mechanism. Miller [114] has also carried out a study on oxyethylated anionic surfactants. The purpose of this work was to address the problem of surfactant purity and also to investigate the experimental methods used to measure the surface tension. Although they conclude that a diffusion-controlled model fits their data well, at long surface lifetimes there is an observed sharp decrease of DST due to surfactant impurities, estimated to be of the order 0.2–0.5%. However, in the time range of validity for Eq. (23) [106], realistic equilibrium surface tensions are obtained by the linear extrapolation, and they conclude that in this time region these equilibrium tension values are not affected by surface active impurities.

On the other hand, homologous di-*n*-alkylsulfates represent a good model system for DST studies, since they can be prepared with a good chain purity and a wide range of hydrophobicities. The general chemical structure of these molecules is given in Fig. 17. The nomenclature is di-C*n*SS where *n* is the length of the carbon chains.

7.1. Equilibrium properties of di-chained sulfosuccinates

As discussed in Section 2, the main impurity for anionic surfactants is believed to be trace di-valent ions, which cause a general lowering of the surface tension. One solution proposed by Thomas et al. for the removal of these surface active divalent cations is to introduce a sequestering agent into the surfactant solution to chelate the divalent ions, rendering them surface-inactive [18]. It is essential that this chelating agent is also not surface active itself. The tetrasodium salt of ethylenediaminetetraacetic acid, (Na_4 EDTA) is a good choice. Thomas et al. believe that once the divalent ions have been removed there is complete consistency between tensiometric and neutron data using a Gibbs prefactor of 2 [15]. This too is still a matter of controversy as the exact levels of these M^{2+} contaminants have not really been identified.

7.1.1. Effect of EDTA on anionic surfactant solutions

Although the surfactants used here were all ion-exchanged on a resin, it was

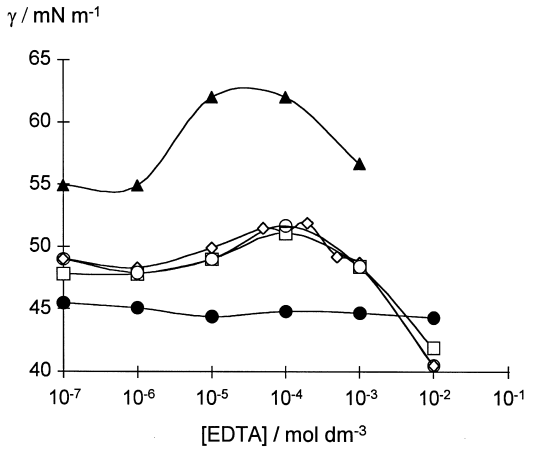

Fig. 18. Effect of various concentrations of EDTA on the surface tensions of a 2×10^{-4} mol dm^{-3} diC6SS solution ( ); a 5×10^{-4} mol dm^{-3} diC6SS solution (□◇○); and a 1×10^{-4} mol dm^{-3} non-ionic glucamide solution (●) as a control.

evident that there were still some divalent ions present. Fig. 18 shows the effect of EDTA on the surface tensions of 5×10^{-4} mol dm^{-3} and 2×10^{-4} mol dm^{-3} diC6SS solutions. At lower EDTA there is no effect on the tension, however, between 10^{-5} and 10^{-4} mol dm^{-3} there is a tension increase, which is consistent with the removal of the divalent ions from the interface. Above EDTA concentra-

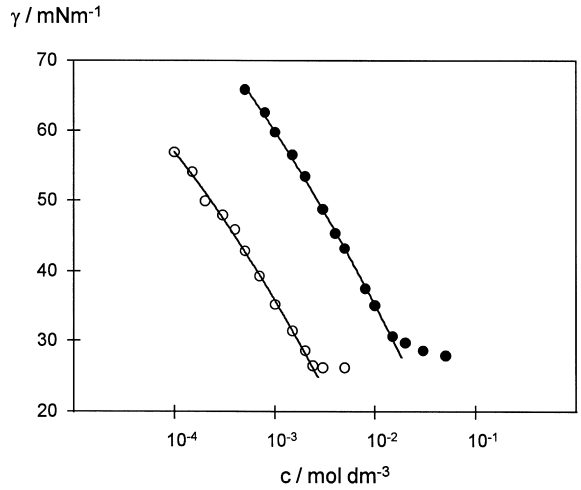

Fig. 19. Equilibrium surface tension vs. concentration plot for diC6SS (●) and diC7SS (○) as measured by drop volume tensiometry. The fit to the pre-CMC data is a quadratic.

tions of $\sim 5 \times 10^{-4}$ mol dm^{-3} there is a lowering of the surface tension due to the partial screening of the electrostatic repulsions between the surfactant head groups — the classical salt effect. This behaviour was also observed for diC7SS.

The effect of EDTA on a di-chained non-ionic surfactant was also investigated as a control, and from Fig. 18 it can be concluded that the effect seen with the anionics are not due to any surface activity of the EDTA.

All equilibrium and dynamic tension measurements carried out were measured at a constant concentration ratio EDTA/surfactant of 1:100, with the EDTA concentration never exceeding 5×10^{-4} mol dm^{-3}, due to the depression of the tension. This concentration ratio was kept constant so that the ratios of the activities of the surfactant solutions also remained constant.

7.1.2. Equilibrium $\gamma - \ln c$ curves for the sulfosuccinates as measured by drop volume tensiometry

Drop volume tensiometry was used for diC6SS and diC7SS, and these curves are shown in Fig. 19. The drop volume technique (LAUDA TVT1) has been outlined by several authors [1,4,115–117], and was used in preference to the du Nouy method owing to greater accuracy and reproducibility. These measurements gave the CMC of diC6SS as 1.3×10^{-2} mol dm^{-3} and diC7SS as 2.0×10^{-3} mol dm^{-3}. The CMC of diC4SS and diC5SS was also measured, but due to their very high CMCs they were less useful for the DST work. The equilibrium surface excess curves Γ_{eq} vs. c for diC6SS and diC7SS are shown in Fig. 20 as determined using the Gibbs equation with a factor of 2.

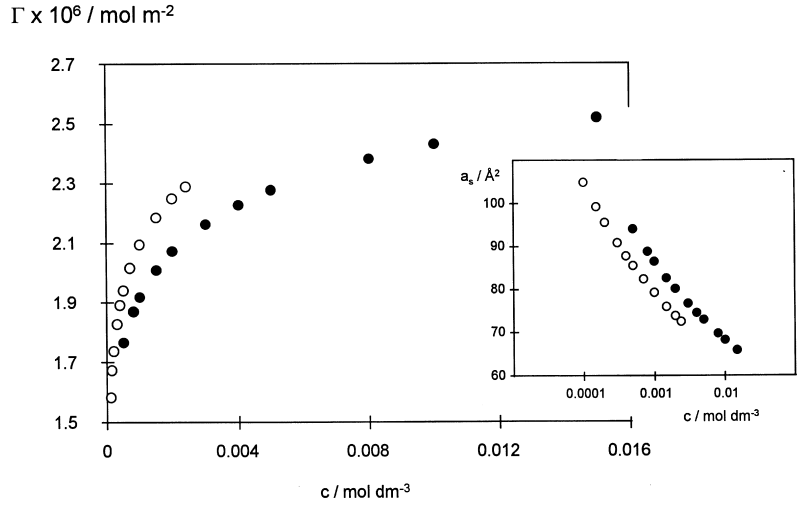

Fig. 20. Equilibrium surface excess Γ_{eq} vs. concentration c for diC6SS (●) and diC7SS (○) as calculated from the Gibbs equation and tensiometric data. Inset shows effective area per molecule at the interface.

7.2. DST as a function of concentration

Analysis of these DST curves at long and short times using Eqs. (20) and (23) gave similar behaviour as for the non-ionics described in Section 5. At short times the process appears to be essentially diffusion-controlled, and at the end the DSTs are consistent with an adsorption barrier, similar in magnitude to that of the non-ionics. This suggests that the DST mechanism is not strongly affected by the chemical nature of the surfactant. However, it is difficult to conclude from the study of these surfactants whether the charged interface has any major effect on the dynamics of adsorption, or not, and further work is needed to clarify this point.

Charge effects have also been considered from a theoretical viewpoint by MacLeod and Radke [118], who concluded that for anionic surfactants the rates of adsorption are approximately an order of magnitude lower than similar non-ionics under similar conditions. This can be thought of as anionics having a larger adsorption barrier than non-ionics, although such striking differences were not obvious from this work. Section 7.3 investigates the effect of added electrolyte on DST decays of anionic surfactants.

7.3. Dynamic surface tension as a function of electrolyte concentration

For diC7SS, at 5×10^{-4} mol dm^{-3}, DST curves as a function of NaCl concentration between 0.002 and 0.1 mol dm^{-3}, are shown in Fig. 21. At salt concentra-

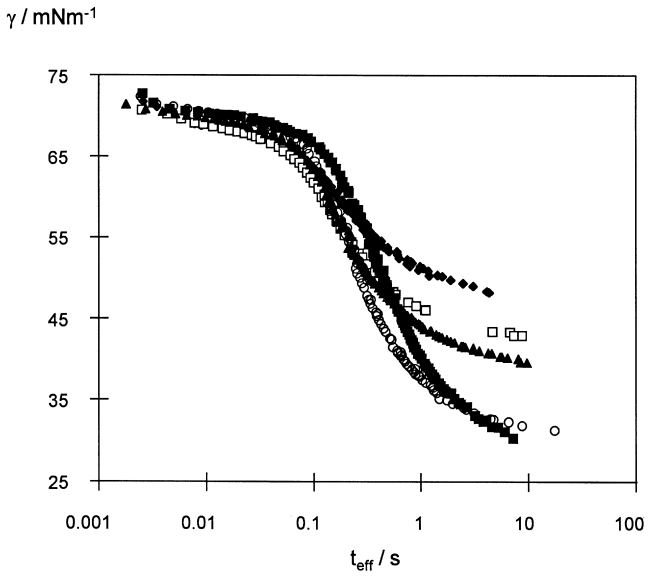

Fig. 21. DST of diC7S at 5×10^{-4} mol dm^{-3} as a function of added electrolyte. [NaCl]/mol dm^{-3}: 0.002 (♦); 0.005 (□); 0.01 (▲); 0.05 (○); 0.1 (■).

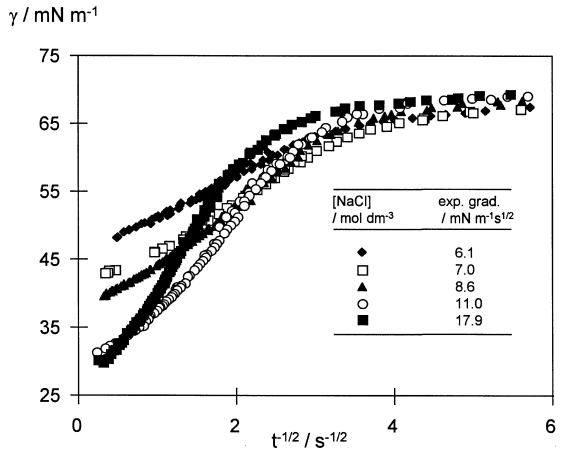

Fig. 22. DST of Fig. 21 plotted against $t^{-1/2}$ to give the long time gradients [Eq. (23)]. Symbols are the same electrolyte concentrations as Fig. 21.

tions lower than 0.002 mol dm^{-3} there were no obvious effects on the DSTs, and for NaCl higher than 0.1 mol dm^{-3} the surfactant was insoluble. With reference to Fig. 21 at the beginning all decays are similar.

Although the surfactant concentration remains constant, the salt concentration has a profound effect on γ_{eq}, and this is seen at the end of the DST decay.

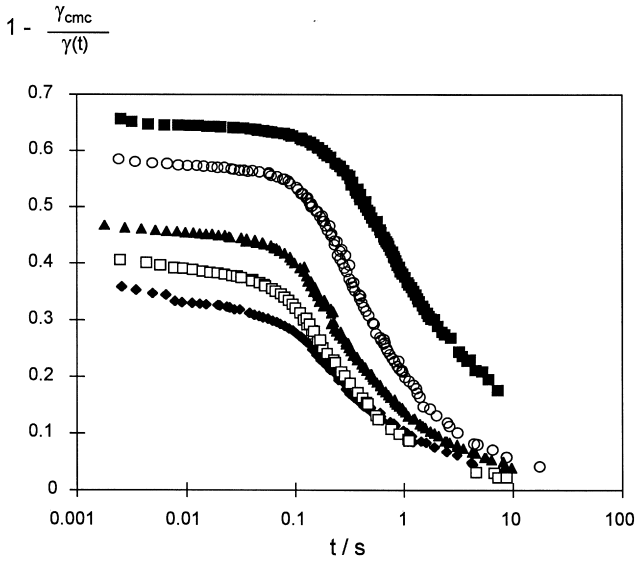

Fig. 23. Reduced DST of data shown in Fig. 21. Electrolyte concentrations and symbols are the same as Fig. 21.

The surface excess as a function of salt concentration has not been measured, however, it would be expected that the value of Γ_{eq} would not change by more than a factor of 2 over the range of salt concentration (in accordance with the Gibbs equation). Long time experimental gradients obtained by plotting γ vs. $t^{-1/2}$ are shown and given in Fig. 22, however, owing to uncertainties in Γ_{eq} it is not possible to take the analysis any further.

It can be seen from the table that the gradient increases significantly as the salt concentration increases, and this would indicate that the effective diffusion coefficient is becoming smaller [Eq. (23)], with therefore the activation barrier becoming larger. This is illustrated more clearly in Fig. 23 where the reduced dynamic surface tension of these solutions have been plotted against time. The reduced DST is defined as $[(\gamma(t) - \gamma_{cmc})/\gamma(t)]$, which enables all values of γ_{cmc} to be re-scaled to the same value, here zero. It is evident that the higher the electrolyte concentration, the higher the surface tension at a certain time, and the longer it takes to reach a reduced tension of zero.

8. Direct measurement of $\Gamma(t)$ by neutron reflection

Recently Bain et al. [119] have studied DSTs of CTAB (cetyltrimethylammonium bromide) solutions using an overflowing cylinder (OFC) method. The dynamic surface tensions were measured using two complementary, non-invasive spectroscopic methods, surface light scattering (SLS) [120] and ellipsometry [121], as well as the traditional Wilhelmy plate.

When the OFC surfactant solution is pumped upwards through a cylinder, the liquid flows radially outwards from the centre to the rim, thereby creating a fresh surface. At steady state, this surface has an expansion rate typically in the range 1–10 s^{-1}[122–124]. The OFC offers a relatively large ($\sim$ 75 cm^2) flat surface, enabling ellipsometric, spectroscopic and other scattering measurements to be performed. Ellipsometry measures the polarisation of light reflected from a liquid surface and is dependent on the thickness of the adsorbed layer and its refractive index. The polarisation can be related to the surface excess of the surfactant solution. The main use is being combined with the overflowing cylinder or inclined plate, so that both γ and Γ can be measured [125].

From these dynamic measurements on CTAB it was seen that for an approximate surface age ($\tau \approx 0.1$ s) on the OFC the three independent methods agreed well with each other. Fig. 24 shows the DST measured by SLS and ellipsometry on the OFC at various CTAB concentrations, at the surface age of approximately 0.1 s. The equilibrium surface tensions of the solutions measured by du Nouy ring and are also shown. As expected the DSTs measured by SLS and ellipsometry are higher than those measured at equilibrium.

Bain et al. have also reported $\Gamma_{dyn}(t)$ measurements of CTAB using this OFC in conjunction with neutron reflection (NR) [126]. The major advantage of this approach is that of $\Gamma_{dyn}(t)$ can be measured directly, rather than invoking an isotherm equation. The measurements were carried out on the SURF reflectome-

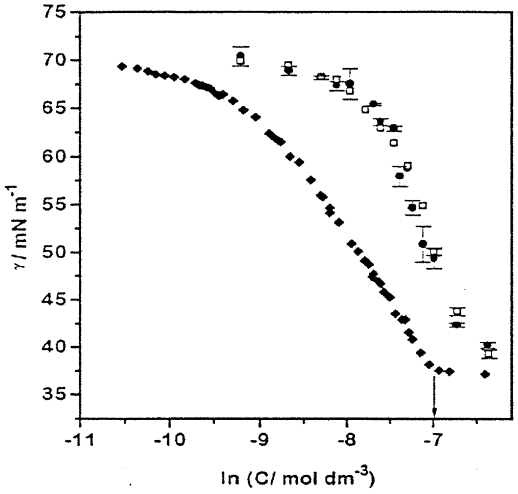

Fig. 24. DST of CTAB at $t \sim 0.1$ s measured by SLS (●) and ellipsometry (□). γ_{eq} measured by du Nouy ring (♦) is also shown. Figure taken from [119], with permission from the American Chemical Society.

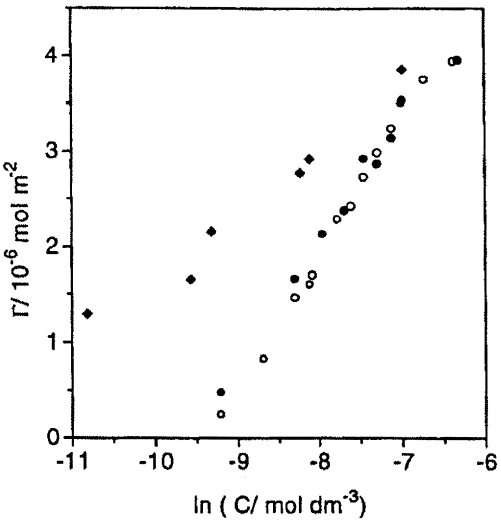

Fig. 25. The dynamic surface excess (●) and equilibrium surface excess (♦) for solutions of CTAB measured by neutron reflection. Dynamic surface excess has also been measured by ellipsometric measurements (○). Reproduced from [126] with permission from the American Chemical Society.

ter at ISIS, UK, and the application NR to surfactant solutions was discussed in Section 2. Using deuterated CTAB layers on null reflecting water (nrw) gave a good enough signal-to-noise to measure areas per molecule down to 300 Å^2. Fig. 25 compares the values of Γ_{dyn}, the surface concentration at ~ 0.1 s, with static measurements of Γ_{eq} obtained by Lu et al. [127] from neutron reflection. Values of Γ_{dyn} obtained were lower than Γ_{eq}, as would be expected when measuring the surface excess before surface equilibrium has been reached. The NR data were in good agreement with adsorbed amounts from the ellipsometry. This exciting work is an important contribution to adsorption dynamics, as it is the first attempt at measuring the dynamic surface excess directly using neutrons.

9. Conclusions and outlook

The field of adsorption kinetics has advanced significantly over the past 10 years. This has mainly been due to an advancement of many of the techniques and also to the better understanding of the equilibrium properties of the surfactants. It is our opinion that a clearer picture of adsorption dynamics is obtained if simple and well characterised surfactants are carefully chosen for study. This is highlighted by concentrating on simple non-ionics. Although there are still cases of diffusion-only controlled adsorption for certain surfactants, many authors now believe that activated diffusion (mixed kinetics) is a better model for most DST data. The pioneering work by Joos, Miller, Fainerman and Makievski on diffusional adsorption has been built on by Liggeiri et al. to incorporate adsorption barriers and activation energies, and evidence for these barriers has been observed by Lin et al. and Eastoe et al. in studies of non-ionic surfactants. The origin of this adsorption barrier may that the molecules must be oriented favourably and/or do work against the surface pressure. In the absence of any molecular theory for DST, an activation barrier can be used to account for all these possibilities, since only molecules with a sufficient energy E_a can adsorb into the layer and effect the tension. It is hoped that from these new experimental results a fresh theoretical effort to understand the origin of this adsorption barrier will be proposed.

When considering ionic surfactants, the question of purity has to be addressed and this has been investigated by Miller et al. on studies of oxyethylated surfactants. This purity problem has also been addressed in this review on studies of sulfosuccinate surfactants (Aerosol-OT analogues).

Most reports on adsorption dynamics in the literature measure $\gamma(t)$ and use an appropriate isotherm to obtain $\Gamma(t)$, however, the model assumptions can lead to errors in these calculated values of the surface excess. This problem has been overcome by Bain et al. [126], who measured $\Gamma(t)$ directly using an overflowing cylinder in conjunction with neutron reflection. They successfully showed that the dynamic surface excess of CTAB could be measured in the time range the OFC permitted. Continuation in this challenging area will enable $\Gamma(t)$ to be measured over a larger time-window and will lead to a greater understanding of the adsorption mechanism. Neutron reflection also gives direct structural information

on the adsorbed layer, and this could give further insight into dynamic film properties.

There is still relatively little research carried out on the effect of temperature on DST, and we feel that these are key experiments for investigating the adsorption mechanisms. Recent experiments on normal C_nE_m non-ionics [66] suggest that the presence of micelles does not significantly affect the DST, at least up to 100 × CMC. However, more experimental work is needed to see if surfactant solutions containing a high concentration of large and stable micelles have any effect on DST. The theoretical works of Joos and Fainerman can also be investigated for these systems.

From an experimental and theoretical point of view, many of the fundamentals of DST and adsorption dynamics for surfactants are now understood. However, it is clear that a combination tensiometry and neutron reflection on dynamic films will place the subject on a firm quantitative footing, and efforts should be concentrated in this area. These experiments, for a range of systems and conditions, would give much better insight into the adsorption mechanism than can be obtained by tensiometry alone.

Nomenclature

CMC:	Critical micelle concentration
C_nE_m:	*n*-Alkyl polyglycol ether of alkyl length n and ethylene oxide length m
CTAB:	Cetyltrimethylammonium bromide
c:	Concentration
c_s:	Concentration in the subsurface
D:	Monomer diffusion coefficient
D_{eff}:	Effective monomer diffusion coefficient
di-(Cn–Glu):	Di-chained glucamide surfactant of single chain length n
diCnSS:	Di-chained sulfosuccinate surfactant of single chain length n
DST:	Dynamic surface tension
E_a:	Activation energy
EDTA:	Ethylenediaminetetraacetic acid
j_{ads}:	Flux of adsorbing monomer
j_{des}:	Flux of desorbing monomer
k_{mic}:	First-order micelle dissociation rate constant
NMR:	Nuclear magnetic resonance
MBP:	Maximum bubble pressure
PFGSE-NMR:	Pulsed field gradient spin echo
R:	Gas constant (= 8.314 J K^{-1} mol^{-1})
SLS:	Surface light scattering
γ,γ_{CMC}:	Surface tension and surface tension at the CMC
γ_{eq}, $\gamma(t)$:	Equilibrium surface tension, surface tension as a function of time
γ_0:	Surface tension of a solvent, here water

Γ, Γ_{eq}:	Surface excess and equilibrium surface excess of surfactant
Γ_{∞}:	Maximum adsorbed amount
$\Gamma(t)$, Γ_{dyn}:	Surface excess measured as a function of time
π:	The surface pressure or pi (3.142..)
τ_1:	Relaxation time for monomer exchange in micelles
τ_2:	Relaxation time for complete micelle dissociation

Acknowledgements

We thank the EPSRC for funding the dynamic surface tension, and studentship to JSD. (GR/K04774 and GR/K85247).

References

[1] S.S. Dukhin, G. Kretzschmar, R. Miller, Dynamics of Adsorption at Liquid Interfaces, Elsevier, Amsterdam, 1995.
[2] A.I. Rusanov, V.A. Prokhorov, Interfacial Tensiometry, Elsevier, Amsterdam, 1996.
[3] C.-H. Chang, E.I. Franses, Colloid Surf. 100 (1995) 1.
[4] R. Miller, P. Joos, V. Fainermann, Adv. Colloid Interface Sci. 49 (1994) 249.
[5] J.W. Gibbs, in: H.A. Bumstead, R.G. van Name (Eds.), Papers of J. Willard Gibbs, 2 vols., Longmans Green, London, 1906 (Reprinted by Dover, New York, 1961).
[6] J.E. Bradley, E.M. Lee, R.K. Thomas et al., Langmuir 4 (1988) 821.
[7] J. Penfold, R.K. Thomas, J. Phys. Condens. Mat. 2 (1990) 1369.
[8] J.R. Lu, E.A. Simister, R.K. Thomas, E.M. Lee, A.R. Rennie, J. Penfold, Langmuir 8 (1992) 1837.
[9] R.K. Thomas, J.R. Lu, E.M. Lee, J. Penfold, S.L. Flitsch, Langmuir 9 (1993) 1352.
[10] J. Eastoe, in: E. Dickinson (Ed.), New Physico-Chemical Techniques for the Characterisation of Complex Food Systems, Chapter 12, Blackie Academic and Professional, London, 1995.
[11] J.R. Lu, Z.X. Li, R.K. Thomas et al., J. Phys. Chem. 98 (1994) 6559.
[12] J.R. Lu, E.M. Lee, R.K. Thomas, J. Penfold, S.L. Flitsch, Langmuir 9 (1993) 1352.
[13] J.R. Lu, T.J. Su, Z.X. Li et al., J. Phys. Chem. B 101 (1997) 10332.
[14] R.K. Thomas, B.P. Binks, J. Penfold et al., J. Phys. Chem. B. 102 (1998) 5785.
[15] S.W An, J.R. Lu, R.X. Thomas, J. Penfold, Langmuir 12 (1996) 2446.
[16] Z.X. Li, E.M. Lee, R.X. Thomas, J. Penfold, J. Colloid Interface Sci. 187 (1997) 492.
[17] Z.X. Li, J.R. Lu, R.K. Thomas, J. Penfold, J. Phys. Chem., B 101 (1997) 1615.
[18] Z.X. Li, J.R. Lu, R.K. Thomas, Langmuir 13 (1997) 3681.
[19] R. Miller, Colloid Polym. Sci. 259 (1981) 375.
[20] V.B. Fainerman, R. Miller, Langmuir 12 (1996) 6011.
[21] W. Henry, Nicholson's J. 4 (1901) 224.
[22] I. Langmuir, Phys. Rev. 8 (1916) 2.
[23] I. Langmuir, Proc. Natl. Acad. Sci. 3 (1917) 141.
[24] I. Langmuir, J. Am. Chem. Soc. 15 (1918) 75.
[25] B. von Szyskowski, Z. Phys. Chem. 64 (1908) 385.
[26] P.W. Atkins, Physical Chemistry, 5 edn, Oxford University Press, Oxford, 1994.
[27] A. Frumkin, Z. Phys. Chem. 116 (1925) 466.
[28] R.P. Borwankar, D.T. Wasan, Chem. Eng. Sci. 43 (1988) 1323.
[29] M. Volmer, Z. Phys. Chem. 115 (1925) 253.
[30] R. Aveyard, D.A. Hayden, An Introduction to the Principles of Surface Chemistry, Cambridge University Press, 1973.

[31] R.P. Borwankar, D.T. Wasan, Chem. Eng. Sci. 41 (1986) 199.
[32] K. Lunkenheimer, R. Hirte, J. Phys. Chem. 96 (1992) 8683.
[33] K. Lunkenheimer, G. Czichocki, R. Hirte, W. Barzyk, Colloid Surf. A. 101 (1995) 187.
[34] A. Dupré, Theorie Mecanique de la Chaleur, Gauthier-Villars, Paris, 1869.
[35] J.W. Gibbs, The Collected Works. vol. 1, Longmans, Green and Co., New York, 1928.
[36] Lord Rayleigh, Proc. R. Soc. 47 (1890) 281.
[37] S.R. Milner, Philos. Mag. Ser. 6 (13) (1907) 96.
[38] R.T. Florence, R.J. Myers, W.D. Harkins, Nature 138 (1936) 200.
[39] N.K. Adam, H.L. Shute, Trans. Faraday Soc. 31 (1935) 205.
[40] N.K. Adam, H.L. Shute, Trans. Faraday Soc. 34 (1938) 758.
[41] G. Goss, Kolloid-Z. 86 (1939) 205.
[42] A.E. Alexander, Trans. Faraday Soc. 37 (1941) 15.
[43] W.N. Bond, H.O. Puls, Philos. Mag. 7 (24) (1937) 864.
[44] S. Ross, J. Am. Chem. Soc. 67 (1945) 990.
[45] I. Langmuir, V.J. Schaefer, J. Am. Chem. Soc. 59 (1937) 2400.
[46] C.C. Addison, J. Chem. Soc. (1944) 252.
[47] C.C. Addison, J. Chem. Soc. (1944) 477.
[48] C.C. Addison, J. Chem. Soc. (1945) 98.
[49] A.F.H. Ward, L. Tordai, J. Chem. Phys. 14 (1946) 453.
[50] K.J. Mysels, A. Florence, J. Colloid Interface Sci. 43 (1973) 577.
[51] K. Lunkenheimer, R. Miller, Tenside Deterg. 16 (1979) 312.
[52] K. Lunkenheimer, R. Miller, H. Fruhner, Colloid Polym. Sci. 260 (1982) 59.
[53] K. Lunkenheimer, R. Miller, J. Colloid Interface Sci. 120 (1987) 176.
[54] V.B. Fainerman, R. Miller, P. Joos, Colloid Polym. Sci. 272 (1994) 731.
[55] R.S. Hansen, J. Phys. Chem. 64 (1960) 637.
[56] R.S. Hansen, J. Colloid Sci. 16 (1961) 585.
[57] K.L. Sutherland, Aust. J. Sci. Res. A 5 (1952) 683.
[58] V.B. Fainerman, A.V. Makievski, R. Miller, Colloid Surf. A. 87 (1994) 61.
[59] J.F. Baret, J. Phys. Chem. 72 (1968) 2755.
[60] F. Ravera, L. Liggieri, A. Steinchen, J. Colloid Interface Sci. 156 (1993) 109.
[61] L. Liggieri, F. Ravera, A. Passerone, Colloid Surf. A. 114 (1996) 351.
[62] S.-Y. Lin, T.-L. Lu, W.-B. Hwang, Langmuir 11 (1995) 555.
[63] S.-Y. Lin, R.-Y. Tsay, L.-W. Lin, S.-I. Chen, Langmuir 12 (1996) 6530.
[64] H.-C. Chang, C.-T. Hsu, S.-Y. Lin, Langmuir 14 (1998) 2476.
[65] J. Eastoe, J.S. Dalton, P.G.A. Rogueda, D. Sharpe, J. Dong, J.R.P. Webster, Langmuir 12 (1996) 2706.
[66] J. Eastoe, J.S. Dalton, P.G.A. Rogueda, E.R. Crooks, A.R. Pitt, E.A. Simister, J. Colloid Interface Sci. 188 (1997) 423.
[67] J. Eastoe, J.S. Dalton, P.G.A. Rogueda, P.C. Griffiths, Langmuir 14 (1998) 979.
[68] J. Eastoe, J.S. Dalton, R.K. Heenan, Langmuir 14 (1998) 5719.
[69] F. MacRitchie, A.E. Alexander, J. Colloid Sci. 18 (1963) 453.
[70] F. MacRitchie, A.E. Alexander, J. Colloid Sci. 18 (1963) 458.
[71] F. MacRitchie, A.E. Alexander, J. Colloid Sci. 18 (1963) 464.
[72] D. Cho, G. Narsimhan, E.I. Franses, J. Colloid Interface Sci. 191 (1997) 312.
[73] S.-U. Um, E. Poptoshev, R.J. Pugh, J. Colloid Interface Sci. 193 (1997) 41.
[74] C. Ybert, J.-M. di Meglio, Langmuir 14 (1998) 471.
[75] B.V. Zhmud, E. Poptoshev, R.J. Pugh, Langmuir 14 (1998) 3620.
[76] A.V. Makievski, V.B. Fainerman, M. Bree, R. Wustneck, J. Kragel, R. Miller, J. Phys. Chem. B. 102 (1998) 417.
[77] J. Lucassen, J. Chem. Soc. Faraday Trans. 1 (72) (1976) 76.
[78] R. Miller, Colloid Polym. Sci. 259 (1981) 1124.
[79] E. Rillaerts, P. Joos, J. Phys. Chem. 86 (1982) 3471.
[80] C.D. Dushkin, I.B. lvanov, P.A. Kralchevsky, Colloid Surf. 60 (1991) 235.
[81] V.B. Fainerman, Colloid Surf. 62 (1992) 333.
[82] V.B. Fainerman, A.V. Makievski, Kolloid Z. (English) 54 (1992) 890.

[83] V.B. Fainerman, A.V. Makievski, Kolloid Z. (English) 54 (1992) 897.
[84] V.B. Fainerman, A.V. Makievski, Colloid Surf. 69 (1993) 249.
[85] K.D. Danov, P.M. Vlahovska, T. Horozov et al., J. Colloid Interface Sci. 183 (1996) 223.
[86] X.Y. Hua, M.J. Rosen, J. Colloid Interface Sci. 124 (1988) 652.
[87] M.J. Rosen, X.Y. Hua, J. Colloid Interface Sci. 139 (1990) 397.
[88] X.Y. Hua, M.J. Rosen, J. Colloid Interface Sci. 141 (1991) 180.
[89] M.J. Rosen, Z.H. Zhu, X.Y. Hua, J. Am. Oil. Chem. Soc. 69 (1992) 30.
[90] T. Gao, M.J. Rosen, J. Colloid Interface Sci. 173 (1995) 42.
[91] T. Gao, M.J. Rosen, J. Am. Oil. Chem. Soc. 71 (1994) 771.
[92] T. Gao, M.J. Rosen, J. Colloid Interface Sci. 172 (1995) 242.
[93] M.J. Rosen, L.D. Song, J. Colloid Interface Sci. 179 (1996) 261.
[94] L.K. Filippov, J. Colloid Interface Sci. 163 (1994) 49.
[95] L.K. Filippov, J. Colloid Interface Sci. 164 (1994) 471.
[96] L.K. Filippov, J. Colloid Interface Sci. 182 (1996) 330.
[97] L.K. Filippov, N.L. Filippova, J. Colloid Interface Sci. 178 (1996) 571.
[98] T. Svitova, H. Hoffmann, R.M. Hill, Langmuir 12 (1996) 1712.
[99] S.-Y. Lin, K. McKeigue, C. Maldarelli, Langmuir 7 (1991) 1055.
[100] R. Miller, V.B. Fainerman, K.-H. Schano, A. Hofmann, W. Heyer, Tenside Sur. Det. 34 (1997) 357.
[101] P.C. Griffiths, P. Stilbs, K. Paulson, A.M. Howe, A.R. Pitt, J. Phys. Chem. 101 (1997) 915.
[102] J. Eastoe, P. Rogueda, W.J. Harrison, A.M. Howe, A.R. Pitt, Langmuir 10 (1994) 4429.
[103] J. Eastoe, P. Rogeuda, A.M. Howe, A.R. Pitt, R.K. Heenan, Langmuir 12 (1996) 2701.
[104] D.J. Cooke, J.R. Lu, E.M. Lee, R.K. Thomas, A.R. Pitt, E.A. Simister, J. Phys. Chem. 100 (1996) 10298.
[105] P. Rogueda, Ph.D. Thesis, University of Bristol, UK, 1996.
[106] A.V. Makievski, V.B. Fainerman, R. Miller, M. Bree, L. Liggieri, F. Ravera, Colloid Surf. A 122 (1997) 269.
[107] P.W. Atkins, Physical Chemistry, 5th ed., Oxford University Press, Oxford, 1994.
[108] E.A.G. Aniannson, S.N. Wall, J. Phys. Chem. 78 (1974) 1024.
[109] E.A.G. Aniannson, S.N. Wall, J. Phys. Chem. 79 (1975) 857.
[110] E.A.G. Aniannson, S.N. Wall, M. Almgren et al., J. Phys. Chem. 80 (1976) 905.
[111] J.S. Dalton, Ph.D. Thesis, University of Bristol, 1998, submitted.
[112] F. Tiberg, B. Jonsson, B. Lindman, Langmuir 10 (1994) 3714.
[113] A. Johner, J.F. Joanny, Macromolecules 23 (1990) 5299.
[114] G. Czichocki, A.V. Makievski, V.B. Fainerman, R. Miller, Colloid Surf. A. 122 (1997) 189.
[115] J. Li, V.B. Fainerman, R. Miller, Langmuir 12 (1996) 5138.
[116] Miller et al., J. Colloid Interface Sci., 186 (1997) 40.
[117] Miller et al., J. Colloid Interface Sci., 186 (1997) 149.
[118] C.A. MacLoed, C.J. Radke, J. Colloid Interface Sci. 160 (1993) 435.
[119] S. Manning-Benson, C.D. Bain, R.C. Darton, D. Sharpe, J. Eastoe, P. Reynolds, Langmuir 13 (1997) 5808.
[120] D. Langevin, in: D. Langevin (Ed.), Light Scattering by Liquid Interfaces and Complementary Techniques, Marcel Dekker, New York, 1992.
[121] J. Meunier, in: D. Langevin (Ed.), Light Scattering by Liquid Interfaces and Complementary Techniques, Chapter 17, Marcel Dekker, New York, 1992.
[122] J.F. Padday, Proc. Int. Congr. Surf. Act. (1957) 1.
[123] D.J.M. Bergink-Martens, H.J. Bos, A. Prins, B.C. Schulte, J. Colloid Interface Sci. 138 (1990) 1.
[124] D.J.M. Bergink-Martens, H.J. Bos, A. Prins, J. Colloid Interface Sci. 165 (1994) 221.
[125] S. Manning-Benson, C.D. Bain, R.C. Darton, J. Colloid Interface Sci. 189 (1997) 109.
[126] S. Manning-Benson, S.R.W. Parker, C.D. Bain, J. Penfold, Langmuir 14 (1998) 990.
[127] J.R. Lu, M. Hromadova, E.A. Simister, R.K. Thomas, J. Penfold, J. Phys. Chem. 98 (1994) 11519.